

1 SARS coronavirus ORF8 protein is acquired from SARS-related coronavirus  
2 from greater horseshoe bats through recombination

3

4 Susanna K. P. Lau,<sup>a,b,c,d†</sup> Yun Feng,<sup>e,f†</sup> Honglin Chen,<sup>a,b,c,d †</sup> Hayes K. H. Luk,<sup>d</sup> Wei-Hong  
5 Yang,<sup>e,f</sup> Kenneth S. M. Li,<sup>d</sup> Yu-Zhen Zhang,<sup>e,f</sup> Yi Huang,<sup>d</sup> Zhi-Zhong Song,<sup>e,f</sup> Wang-NGai  
6 Chow,<sup>d</sup> Rachel Y. Y. Fan,<sup>d</sup> Syed Shakeel Ahmed,<sup>d</sup> Hazel C. Yeung,<sup>d</sup> Carol S. F. Lam,<sup>d</sup>  
7 Jian-Piao Cai,<sup>d</sup> Samson S. Y. Wong,<sup>a,b,c,d</sup> Jasper F. W. Chan,<sup>a,b,c,d</sup> Kwok-Yung Yuen,<sup>a,b,c,d</sup>  
8 Hai-Lin Zhang,<sup>e,f\*</sup> Patrick C. Y. Woo<sup>a,b,c,d\*</sup>

9

10 State Key Laboratory of Emerging Infectious Diseases,<sup>a</sup> Research Centre of Infection and  
11 Immunology,<sup>b</sup> Carol Yu Centre for Infection,<sup>c</sup> Department of Microbiology,<sup>d</sup> The  
12 University of Hong Kong, Hong Kong, China; Yunnan Institute of Endemic Diseases  
13 Control and Prevention,<sup>e</sup> Yunnan Provincial Key Laboratory for Zoonosis Control and  
14 Prevention,<sup>f</sup> Dali, Yunnan, China

15

16 Running title: Origin of SARS coronavirus ORF8

17

18 <sup>†</sup>SKP Lau, Y Feng and H Chen contributed equally to the manuscript.

19

20 \*Corresponding authors. Mailing address: Patrick CY Woo, State Key Laboratory  
21 of Emerging Infectious Diseases, Department of Microbiology, The University of Hong  
22 Kong, Room 423, University Pathology Building, Queen Mary Hospital, Hong Kong,  
23 China. E-mail: [pcywoo@hku.hk](mailto:pcywoo@hku.hk); Hai-Lin Zhang, Yunnan Institute of Endemic Diseases

24 Control and Prevention, Dali, Yunnan 671000, PR China. E-mail:

25 [zhangHL715@163.com](mailto:zhangHL715@163.com)

26

27 Abstract: 248 words

28 Text: 5315 words

29

30 **ABSTRACT**

31 Despite the identification of horseshoe bats as the reservoir of SARS-related-  
32 coronaviruses (SARSr-CoVs), the origin of SARS-CoV ORF8, which contains the 29-nt  
33 signature deletion among human strains, remains obscure. Although two SARSr-Rs-  
34 BatCoVs, RsSHC014 and Rs3367, previously detected from Chinese horseshoe bats  
35 (*Rhinolophus sinicus*) in Yunnan, possessed 95% genome identities to human/civet  
36 SARSr-CoVs, their ORF8 exhibited only 32.2-33% aa identities to that of human/civet  
37 SARSr-CoVs. To elucidate the origin of SARS-CoV ORF8, we sampled 348 bats of  
38 various species in Yunnan, among which diverse *alphacoronaviruses* and  
39 *betacoronaviruses*, including potentially novel CoVs, were identified, with some showing  
40 potential interspecies transmission. The genomes of two *betacoronaviruses*, SARSr-Rf-  
41 BatCoV YNLF\_31C and YNLF\_34C, from greater horseshoe bats (*Rhinolophus*  
42 *ferrumequinum*), possessed 93% nt identities to human/civet SARSr-CoV genomes.  
43 Although they displayed lower similarities to civet SARSr-CoVs than SARSr-Rs-  
44 BatCoV RsSHC014 and Rs3367 in S protein, their ORF8 demonstrated exceptionally  
45 high (80.4-81.3%) aa identities to that of human/civet SARSr-CoVs, compared to  
46 SARSr-BatCoVs from other horseshoe bats (23.2-37.3%). Potential recombination events  
47 were identified around ORF8 between SARSr-Rf-BatCoVs and SARSr-Rs-BatCoVs,  
48 leading to the generation of civet SARSr-CoVs. The expression of ORF8 subgenomic  
49 mRNA suggested that this protein may be functional in SARSr-Rf-BatCoVs. The high  
50 Ka/Ks ratio among human SARS-CoVs compared to SARSr-BatCoVs supported that  
51 ORF8 is under strong positive selection during animal-to-human transmission. Molecular  
52 clock analysis using ORF1ab showed that SARSs-Rf-BatCoV YNLF\_31C and

53 YNLF\_34C diverged from civet/human SARSr-CoVs at approximately 1990. SARS-  
54 CoV ORF8 is originated from SARSr-CoVs of greater horseshoe bats through  
55 recombination, which may be important for animal-to-human transmission.  
56

57 **IMPORTANCE**

58 Although horseshoe bats are the primary reservoir of *SARS-related-coronaviruses*  
59 (SARSr-CoVs), it is still unclear how these bat viruses have evolved to cross the species  
60 barrier to infect civet/human. Most human SARS-CoV epidemic strains contained a  
61 signature 29-nt deletion in ORF8 compared to civet SARSr-CoVs, suggesting that ORF8  
62 may be important for interspecies transmission. However, the origin of SARS-CoV ORF8  
63 remains obscure. In particular, SARSr-Rs-BatCoVs from Chinese horseshoe bats  
64 exhibited <40% aa identities to human/civet SARS-CoV in ORF8. We detected diverse  
65 *alphacoronaviruses* and *betacoronaviruses* among various bat species in Yunnan,  
66 including two SARSr-Rf-BatCoVs from greater horseshoe bats that possessed an ORF8  
67 with exceptionally high aa identities to that of human/civet SARSr-CoVs. We  
68 demonstrated recombination events around ORF8 between SARSr-Rf-BatCoVs and  
69 SARSr-Rs-BatCoVs, leading to the generation of civet SARSr-CoVs. Our findings offer  
70 insight into the evolutionary origin of SARS-CoV ORF8 which was likely acquired from  
71 SARSr-CoVs of greater horseshoe bats through recombination.

72

## 73 INTRODUCTION

74 Coronaviruses (CoVs) are known to cause respiratory, enteric, hepatic and neurological  
75 diseases of varying severity in a variety of animals. They are currently classified into four  
76 genera, *Alphacoronavirus*, *Betacoronavirus*, *Gammacoronavirus* and *Deltacoronavirus*,  
77 replacing the traditional three groups, group 1 to 3 (1-4). The genus *Betacoronavirus* is  
78 further classified into lineages A to D (3, 5, 6). Among CoVs that infect humans, *human*  
79 *CoV 229E* (HCoV 229E) and *human CoV NL63* (HCoV NL63) belong to  
80 *Alphacoronavirus*; *human CoV OC43* (HCoV OC43) and *human CoV HKU1* (HCoV  
81 HKU1) belong to *Betacoronavirus* lineage A; *Severe Acute Respiratory Syndrome-*  
82 *related CoV* (SARSr-CoV) belongs to *Betacoronavirus* lineage B; and the recently  
83 emerged *Middle East Respiratory Syndrome CoV* (MERS-CoV) belongs to  
84 *Betacoronavirus* lineage C (7-16). The high recombination rate, coupled with the  
85 infidelity of the RNA-dependent RNA polymerase (RdRp), may have facilitated CoVs to  
86 adapt to new hosts and ecological niches, causing epidemics in animals and humans (5,  
87 17-24).

88 The SARS epidemic and identification of SARSr-CoVs from palm civet and  
89 horseshoe bats in China have boosted interests in the discovery of novel CoVs in both  
90 humans and animals especially bats (25-29). With the exception of lineage A  
91 *betacoronaviruses*, bats are now known to be an important reservoir of diverse  
92 *alphacoronaviruses* and lineage B, C and D *betacoronaviruses* (30-38), with bat CoVs  
93 being the gene source for other mammalian CoVs (4). In particular, the findings of bat  
94 CoVs related to SARS-CoV and MERS-CoV suggested that bats may be the animal  
95 origin of both SARS and MERS epidemics; while other animals have served as the

96 intermediate or amplifying hosts for animal-to-human transmission, palm civets in the  
97 case of SARS and dromedary camels in MERS (25, 27, 28, 39-41). However, the  
98 evolutionary paths from bat CoVs to CoVs capable of infecting intermediate hosts and  
99 humans are not fully understood.

100 SARSr-CoVs have been detected in at least 11 different species of horseshoe bats  
101 (genus *Rhinolophus*) from various countries in Asia, Africa and Europe (27, 28, 35, 37,  
102 38, 42, 43). Related viruses have also been reported in bats of other genera, such as  
103 *Chaerophon* and *Hipposideros*, from Africa and China (43-45). However, it is still  
104 unclear how these bat CoVs have evolved to generate the ancestor of civet/human  
105 SARSr-CoVs capable of crossing the species barrier. The genome organization of  
106 SARSr-CoVs, similar to other CoVs, possessed the characteristic gene order 5'-open  
107 reading frame 1ab (ORF1ab), spike (S), ORF3, envelope (E), membrane (M), ORF 6 to 8,  
108 nucleocapsid (N)-3'. It is known that most human SARS-CoVs during the epidemic  
109 contained a signature 29-nt deletion in ORF8 compared to civet SARSr-CoVs (25),  
110 suggesting that this genomic region may be important for interspecies transmission.  
111 However, the origin of SARS-CoV ORF8 remains obscure. Genomes of SARS-related  
112 *Rhinolophus sinicus* BatCoVs (SARSr-Rs-BatCoVs), previously designated SARSr-Rh-  
113 BatCoVs, from Chinese horseshoe bats (*Rhinolophus sinicus*) in Hong Kong and the  
114 Guangdong Province only shared 87-92% nucleotide (nt) identities to human/civet  
115 SARSr-CoV genomes (22, 27, 28). A subsequent study identified two SARSr-Rs-  
116 BatCoVs, RsSHC014 and Rs3367, in the Yunnan Province, which were more closely  
117 related to human/civet SARSr-CoVs (with 95% genome sequence identities) than any  
118 other SARSr-BatCoVs (42). The S proteins of these two SARSr-Rs-BatCoVs from

119 Yunnan shared 90.1-92.3% amino acid (aa) identities to those of human/civet SARSr-  
120 CoVs, compared to 79-80% aa identities between SARSr-Rs-BatCoVs from Hong Kong  
121 and human/civet SARSr-CoVs (27, 42). Moreover, a highly similar virus, SARSr-Rs-  
122 BatCoV WIV1, isolated in Vero E6 cells, was able to use angiotensin converting enzyme  
123 II (ACE2) from humans, civets, and Chinese horseshoe bats as receptor for cell entry,  
124 suggesting that intermediate hosts between bats and human/civets may not be necessary  
125 for interspecies transmission (42). However, considerable genetic distance still exists  
126 between the two SARSr-Rs-BatCoVs from Yunnan and human/civet SARSr-CoVs,  
127 especially in the ORF8 region with only 32.2-33% aa identities.

128 To elucidate the evolutionary origin of SARS-CoV ORF8 and search for even  
129 closer bat CoV ancestors of SARS-CoV, we conducted a three-month study (May to July  
130 2013) on CoVs among various bats from different regions of the Yunnan Province.  
131 Diverse CoVs were detected, including two SARS-related *Rhinolophus ferrumequinum*  
132 BatCoVs (SARSr-Rf-BatCoVs) from greater horseshoe bats (*Rhinolophus*  
133 *ferrumequinum*), which possessed an expressed ORF8 much more closely related to  
134 human/civet SARSr-CoVs than CoVs detected from other bat species. Recombination  
135 and molecular clock analysis were also performed to elucidate the evolutionary paths and  
136 time of interspecies transmission of SARSr-CoVs.



137 **MATERIALS AND METHODS**

138 **Ethics statement.** The collection of bat samples was approved and performed by the  
139 Yunnan Institute of Endemic Diseases Control and Prevention, Dali, Yunnan, China. All  
140 bats were maintained and handled using standard procedures approved by the Medical  
141 Ethical Committee of Yunnan Institute of Endemic Diseases Control and Prevention,  
142 China.

143 **Sample collection.** Bats were captured from various locations in five counties of  
144 four prefectures of the Yunnan Province, China from May to July 2013 (Fig. 1). Samples  
145 were collected using procedures described previously (27, 46). All samples were placed  
146 in viral transport medium (Earle's balanced salt solution, 0.09% glucose, 0.03% sodium  
147 bicarbonate, 0.45% bovine serum albumin, 50 mg/ml amikacin, 50 mg/ml vancomycin,  
148 40 U/ml nystatin) and stored at -80°C before RNA extraction.

149 **RNA extraction.** Viral RNA was extracted from alimentary samples using  
150 QIAamp Viral RNA Mini Kit (QIAGEN, Hilden, Germany). The RNA was eluted in 50 µl  
151 of AVE buffer and was used as the template for RT-PCR.

152 **RT-PCR for CoVs and DNA sequencing.** CoVs screening was performed by  
153 amplifying a 440-bp fragment of the RdRp gene of CoVs using conserved primers (5'-  
154 GGTGGGACTATCCTAAGTGTGA-3' and 5'-  
155 ACCATCATCNGANARDATCATNA-3') targeted to RdRp genes of CoVs (12).  
156 Reverse transcription was performed using the SuperScript III kit (Invitrogen, Life  
157 Technologies, Grand Island, NY, USA). The PCR mixture (25 µl) contained cDNA, PCR  
158 buffer (10 mM Tris-HCl pH 8.3, 50 mM KCl, 3 mM MgCl<sub>2</sub> and 0.01% gelatin), 200 µM  
159 of each dNTPs and 1.0 U *Taq* polymerase (Applied Biosystems, Life Technologies,

160 Grand Island, NY, USA). The mixtures were amplified in 40 cycles of 94°C for 1 min,  
161 48°C for 1 min and 72°C for 1 min and a final extension at 72°C for 10 min in an  
162 automated thermal cycler (Applied Biosystems). Standard precautions were taken to  
163 avoid PCR contamination and no false-positive was observed in negative controls.

164 The PCR products were gel-purified using the QIAquick gel extraction kit  
165 (QIAGEN). Both strands of the PCR products were sequenced twice with an ABI Prism  
166 3700 DNA Analyzer (Applied Biosystems), using the two PCR primers. The sequences  
167 of the PCR products were compared with known sequences of the RdRp genes of CoVs  
168 in the GenBank database. Phylogenetic tree was constructed using the 266-bp fragments  
169 of the RdRp gene with maximum likelihood method using substitution model of General  
170 Time Reversible model with Gamma Distribution as well as allowance of evolutionarily  
171 invariable sites (GTR+G+I) by MEGA 5.0 (47).

172 **Viral culture.** The two samples positive for SARSr-Rf-BatCoVs were subject to  
173 virus isolation in Vero E6 (African green monkey kidney) and primary *R. sinicus* lung  
174 cells as described previously (21).

175 **Complete genome sequencing and analysis of SARSr-Rf-BatCoVs.** Two  
176 complete genomes of SARSr-Rf-BatCoVs were amplified and sequenced using RNA  
177 extracted from the alimentary samples as templates. RNA was converted to cDNA by a  
178 combined random-priming and oligo(dT) priming strategy. The cDNA was amplified by  
179 degenerate primers as described previously (27). A total of 75 sets of primers, available  
180 on request, were used for PCR. The 5' end of the viral genome was confirmed by rapid  
181 amplification of cDNA ends using the 5'/3' SMARTer<sup>TM</sup> RACE cDNA Amplification Kit  
182 (Clontech, USA). Sequences were assembled and manually edited to produce the final

183 sequences. The nt sequences of the genomes and the deduced aa sequences of the ORFs  
184 were compared to those of other CoVs using the coronavirus database CoVDB (48).  
185 Phylogenetic tree construction was performed using maximum likelihood method with  
186 MEGA 6.0.

187 **Recombination analysis.** To detect possible recombination between different  
188 SARSr-BatCoVs and civet SARSr-CoVs, sliding window analysis was performed using  
189 nt alignment of the available genome sequences generated by ClustalX version 1.83 and  
190 edited manually with BioEdit version 7.1.3. Similarity Plot analysis and Bootscan  
191 analysis were performed using Simplot version 3.5.1 (49) (F84 model; window size, 1000  
192 bp; step, 200 bp) with civet SARSr-CoV SZ3 as query.

193 **Estimation of synonymous and non-synonymous substitution rates.** The  
194 number of synonymous substitutions per synonymous site,  $K_s$ , and the number of non-  
195 synonymous substitutions per non-synonymous site,  $K_a$ , for each coding region were  
196 calculated for all available SARSr-Rf-BatCoV, SARSr-Rs-BatCoV, civet SARSr-CoV  
197 and human SARSr-CoV genomes using the Nei-Gojobori method (Jukes-Cantor) in  
198 MEGA 5.0.

199 **Estimation of divergence dates.** The tMRCA was estimated based on an  
200 alignment of ORF1ab and nsp5 sequences, using the Uncorrelated exponential distributed  
201 relaxed clock model (UCED) in BEAST version 1.8 (<http://evolve.zoo.ox.ac.uk/beast/>)  
202 (50). Under this model, the rates were allowed to vary at each branch drawn  
203 independently from an exponential distribution. The sampling dates of all strains were  
204 collected from the literature or from the present study, and were used as calibration points.  
205 Depending on the data set, Markov chain Monte Carlo (MCMC) sample chains were run

for  $2 \times 10^8$  states, sampling every 1,000 generations under the GTR nt substitution model, determined by MODELTEST and allowing  $\gamma$ -rate heterogeneity for all data sets. A constant population coalescent prior was assumed for all data sets. The median and HPD were calculated for each of these parameters from two identical but independent MCMC chains using TRACER 1.3 (<http://beast.bio.ed.ac.uk>). The tree was annotated by TreeAnnotator, a program of BEAST and displayed by FigTree (<http://tree.bio.ed.ac.uk/software/figtree/>).

### **Expression of ORF8 and determination of leader-body junction sequence.**

The leader-body junction site and flanking sequences of the ORF8 subgenomic mRNA in SARSr-Rf-BatCoV YNLF\_31C were determined using RT-PCR as described previously (21, 51). Briefly, RNA was extracted directly from the bat samples using TRIzol Reagent (Invitrogen). Reverse transcription was performed using random hexamers and the SuperScript III kit (Invitrogen). cDNA was PCR amplified with a forward primer (5'-CTACCCAGGAAAAGCCAAC-3') located in the leader sequence and a reverse primer (5'-TGAACCATAGTGTGCCATCT-3') located in the body of the ORF8 mRNA. The PCR mixture (25  $\mu$ l) contained cDNA, PCR buffer (10 mM Tris-HCl pH 8.3, 50 mM KCl, 2 mM  $MgCl_2$  and 0.01% gelatin), 200  $\mu$ M of each dNTPs and 1.0 U *Taq* polymerase (Applied Biosystems). The mixtures were amplified in 60 cycles of 94°C for 1 min, 50°C for 1 min and 72°C for 1 min and a final extension at 72°C for 10 min in an automated thermal cycler (Applied Biosystems). RT-PCR products were subject to agarose gel electrophoresis gel-purified using QIAquick gel extraction kit (QIAGEN) and sequenced to obtain the leader-body junction sequences for the ORF8 subgenomic mRNA.

228           **Nucleotide sequence accession numbers.** The nt and genome sequences of the  
229    CoVs detected in this study have been lodged within the GenBank sequence database  
230    under accession no. KP886808, KP886809, and KP895482 to KP895525.

231 **RESULTS**

232 **Detection of CoVs in bats.** A total of 348 alimentary samples from bats belonging to  
233 five different genera were obtained from various regions of the Yunnan province. RT-  
234 PCR for a 440-bp fragment of the RdRp gene of CoVs was positive in alimentary  
235 samples from 46 bats of five species belonging to four genera (Table 1, Fig. 1). Sequence  
236 analysis showed that 35 samples contained diverse *alphacoronaviruses*, while 11 samples  
237 contained *betacoronaviruses*, including two lineage B *betacoronaviruses* and nine  
238 lineage D *betacoronaviruses*.

239 **Detection of diverse bat *alphacoronaviruses*.** Phylogenetic analysis of the 440-  
240 bp fragments of the RdRp gene of *alphacoronaviruses* detected in 35 bat samples showed  
241 that two sequences from one *Rhinolophus steno* and one *Myotis daubentonii* captured in  
242 Mojiang possessed 92-93% nt identities to *Rhinolophus bat CoV HKU2* (Rh-BatCoV  
243 HKU2) (GenBank accession no. NC\_009988.1) (Table 1, Fig. 2). Four sequences from *M.*  
244 *daubentonii* in Xiangyun possessed 81% nt identity to Rh-BatCoV HKU2 (GenBank  
245 accession no. NC\_009988.1). Twenty-four sequences from *M. daubentonii* in Xiangyun  
246 possessed 78-99% nt identities to *Myotis bat CoV HKU6* (My-BatCoV HKU6) (GenBank  
247 accession no. DQ249224.1). Two sequences from *M. daubentonii* in Mojiang possessed  
248 96% nt identities to *Miniopterus bat CoV HKU7* (Mi-BatCoV HKU7) (GenBank  
249 accession no. DQ249226.1). One sequence from *M. daubentonii* in Mojiang possessed  
250 96% nt identities to *Miniopterus bat CoV HKU8* (GenBank accession no. NC\_010438.1).  
251 Two sequences from *Hipposideros Pomona* in Mojiang possessed 81-87% nt identities to  
252 *Hipposideros bat CoV HKU10* (Hi-BatCoV HKU10) (GenBank accession no.  
253 JQ989267.1).

254           **Detection of lineage B and D bat *betacoronaviruses*.** Phylogenetic analysis of  
255 the 440-bp fragments of the RdRp gene of *betacoronaviruses* detected in two bat samples,  
256 YNLF\_31C and YNLF\_34C, showed that they belonged to *Betacoronavirus* lineage B,  
257 with 100% nt identities to human SARS-CoV TOR2 (GenBank accession no.  
258 AY274119.3) and 90% nt identities to SARSr-Rs-BatCoV HKU3 (GenBank accession no.  
259 DQ022305), thus representing SARSr-Rf-BatCoVs (Table 1, Fig. 2). Both samples were  
260 collected from greater horseshoe bats (*Rhinolophus ferrumequinum*) captured in Lufeng  
261 County, Chuxiong Yi Autonomous Prefecture (Fig. 1). Phylogenetic analysis of the 440-  
262 bp fragments of the RdRp gene of *betacoronaviruses* detected in nine other bat samples  
263 showed that they belonged to *Betacoronavirus* lineage D, with 75-79% nt identities to  
264 *Rousettus bat coronavirus HKU9* (Ro-BatCoV HKU9) (GenBank accession no.  
265 NC\_009021.1). These nine samples were collected from Leschenault's rousettes  
266 (*Rousettus leschenaulti*) in Mengla County, Xishuangbanna Dai Autonomous Prefecture.  
267 Attempts to passage SARSr-Rs-BatCoV YNLF\_31C and YNLF\_34C in various cell lines  
268 were not successful, with no cytopathic effect or viral replication being detected.

269           **Genome comparison between SARSr-Rf-BatCoV and other SARSr-CoVs.**

270 The complete genome sequences of the two SARSr-Rf-BatCoV strains, YNLF\_31C and  
271 YNLF\_34C, were obtained by assembly of the sequences of RT-PCR products obtained  
272 directly from alimentary samples. Their genome sizes were 29723 bases, with G + C  
273 content 40.7%, comparable to those of most other SARSr-CoVs (27, 28). They were  
274 closely related to each other with 99.9% overall nt identities, while they possessed 88.2%  
275 nt identities to the genomes of SARSr-Rs-BatCoV HKU3 and 93% nt identities to the  
276 genomes of human/civet SARSr-CoVs. SARSr-Rf-BatCoV strains share similar genome

277 organization with other SARSr-CoV strains, containing the putative transcription  
278 regulatory sequence (TRS) motif, 5'-ACGAAC-3', at the 3' end of the 5' leader sequence  
279 and preceding each ORF except ORF 7b. Similar to most other SARSr-BatCoVs, SARSr-  
280 Rf-BatCoV YNLF\_31C and YNLF\_34C contained a single long ORF8.

281         The nsp3, S, ORF3 and ORF8 regions are known to be the most rapidly evolving  
282 regions among SARSr-CoV genomes (27, 28, 52, 53). Pairwise comparison of aa  
283 sequences between civet SARSr-CoV SZ3 and other SARSr-CoVs showed that the S and  
284 ORF3a of SARSr-Rf-BatCoV YNLF\_31C and YNLF\_34C displayed relatively low  
285 sequence identities to civet SARSr-CoV (Table 2). However, the nsp3 of SARSr-Rf-  
286 BatCoV YNLF\_31C and YNLF\_34C exhibited 97.1% aa identity to civet SARSr-CoV,  
287 which is comparable to the high sequence identity of 96.8 to 97.5% between civet  
288 SARSr-CoV and SARSr-BatCoVs, Rs3367, RsSHC014, WIV1 and BtCoV-Cp/2011,  
289 from Yunnan reported previously (42). Furthermore, an exceptionally high sequence  
290 identity (80.4-81.3% aa identity) was observed in the ORF8 between SARSr-Rf-BatCoVs  
291 and human/civet SARSr-CoVs, much higher than that between human/civet SARSr-  
292 CoVs and other SARSr-BatCoVs (23.2-37.3% aa identity). Therefore, civet SARSr-CoV  
293 SZ3 was most closely related to SARSr-Rs-BatCoV Rs3367 and WIV1 in S and ORF3a,  
294 but was most closely related to SARSr-Rf-BatCoVs in ORF8.

295         The predicted receptor binding domain (RBD) of SARSr-Rf-BatCoV YNLF\_31C  
296 and YNLF\_34C possessed 89% and 68.1% aa identities to that of SARSr-Rs-BatCoV  
297 HKU3-1 and civet SARSr-CoV SZ3 respectively. Previous studies have identified five  
298 critical residues (residues 442, 472, 479, 487 and 491) for ACE2 binding in human and  
299 civet SARSr-CoVs (54). In particular, residues 479 and 487 are the two key residues that



300 are different between human and civet SARSr-CoV strains, with S→T substitution at  
301 residue 487 resulting in 20-fold reduction in human ACE2 binding affinity (54). In  
302 SARSr-Rs-BatCoV Rs3367, two (residues 479 and 491) of the five critical residues were  
303 conserved. In SARSr-Rf-BatCoVs and most other SARSr-Rs-BatCoVs, only residue 491  
304 was conserved (Fig. 3). Compared to human/civet SARSr-CoVs and SARSr-Rs-BatCoV  
305 Rs3367, WIV1 and RsSHC014, the RBD of SARSr-Rf-BatCoV YNLF\_31C and  
306 YNLF\_34C, similar to some SARSr-BatCoV strains, contained two deletions of 5 aa and  
307 12 aa respectively.

308 **Phylogenetic analysis.** Phylogenetic trees were constructed using nsp2, nsp3,  
309 nsp5, nsp12 (RdRp), S, ORF3a, ORF8 and N of SARSr-Rf-BatCoV YNLF\_31C and  
310 YNLF\_34C and other SARSr-CoVs (Fig. 4). These regions were selected because they  
311 were commonly used in phylogenetic analysis of CoVs (RdRp, S, N), represent regions  
312 of rapid evolution in SARSr-CoVs (nsp3, ORF3, ORF8), or free from recombination  
313 upon subsequent analysis (nsp2, nsp5). In nsp2, nsp3, nsp5, RdRp, and N genes, SARSr-  
314 Rf-BatCoV YNLF\_31C and YNLF\_34C were more closely related to other SARSr-  
315 BatCoVs than to two other SARSr-Rf-BatCoV strains, Rf1 and BtCoV/273/2005,  
316 previously detected from greater horseshoe bats in Hubei (28, 37). However, in S, ORF3  
317 and ORF8, SARSr-Rf-BatCoV YNLF\_31C and YNLF\_34C were most closely related to  
318 SARSr-Rf-BatCoV Rf1 and BtCoV/273/2005, forming a distinct cluster among other  
319 SARSr-BatCoVs.

320 In S and ORF3 region, human/civet SARSr-CoVs were most closely related to  
321 SARSr-Rs-BatCoV Rs3367, WIV1 and RsSHC014 previously detected from Yunnan  
322 bats (42). This is in line with the ability of SARSr-Rs-BatCoV WIV1 to replicate in

323 VeroE6 cells and use ACE2 as receptor (42). In nsp3, human/civet SARSr-CoVs were  
324 most closely related to SARSr-Rf-BatCoV YNLF\_31C and YNLF\_34C as well as  
325 SARSr-Rs-BatCoV Rs3367, WIV1 and RsSHC014. Furthermore, in ORF8, SARSr-Rf-  
326 BatCoV strains were clustered with human and civet SARSr-CoV strains with high  
327 bootstrap value of 990, whereas all SARSr-Rs-BatCoV strains, including Rs3367, WIV1  
328 and RsSHC014, formed another cluster. This concurs with results from pairwise aa  
329 sequence comparison, and suggests that the ORF8 of civet and human SARSr-CoV was  
330 originated from SARSr-Rf-BatCoVs from greater horseshoe bats instead of SARSr-Rs-  
331 BatCoV from Chinese horseshoe bats.

332 **Recombination analysis.** Since the ORF8 of SARSr-Rf-BatCoVs showed high  
333 sequence identity to those of human/civet SARSr-CoVs, we hypothesize that the ancestor  
334 of civet SARSr-CoVs has acquired its ORF8 from SARSr-Rf-BatCoVs through  
335 recombination between SARSr-Rf-BatCoVs from greater horseshoe bats and SARSr-Rs-  
336 BatCoVs from Chinese horseshoe bats. When civet SARSr-CoV SZ3 was used as the  
337 query for sliding window analysis with SARSr-Rf-BatCoV YNLF\_31C and SARSr-Rs-  
338 BatCoV Rs3367 and HKU3 as potential parents, several recombination breakpoints were  
339 observed. In particular, two breakpoints, between which ORF8 was located, were  
340 identified (Fig. 5). Downstream to the first breakpoint at position 27128 and upstream to  
341 the second breakpoint at position 28635, an abrupt change in clustering occurred with  
342 high bootstrap support for clustering of civet SARSr-CoV SZ3 with SARSr-Rf-BatCoV  
343 YNLF\_31C. This is in line with results from phylogenetic and similarity plot analysis.  
344 Moreover, using multiple alignments, civet SARSr-CoV SZ3 was shown to possess much  
345 higher sequence similarities to SARSr-Rf-BatCoVs than to SARSr-Rs-BatCoVs within

346 ORF8 which includes the region corresponding to the 29-nt deletion found in human  
347 SARS-CoVs (Fig. 5).

348 Besides ORF8, another region of interest was S which was situated between two  
349 breakpoints at position 20900 and 26100 respectively (Fig. 5). Downstream to position  
350 20900 and upstream to position 26100, an abrupt change in clustering occurred with high  
351 bootstrap support for clustering of civet SARSr-CoV SZ3 with SARSr-Rs-BatCoV  
352 Rs3367. This is in line with phylogenetic analysis and the ability of strain Rs3367 to use  
353 ACE2 as receptor for cellular entry (42). However, similarity plot analysis still showed  
354 substantial difference between the S of civet SARSr-CoV SZ3 and SARSr-Rs-BatCoV  
355 Rs3367, especially in the S1 region.

356 **Estimation of synonymous and non-synonymous substitution rates.** Using all  
357 available SARSr-BatCoV genome sequences for analysis, the Ka/Ks ratios for various  
358 coding regions, as compared to those of civet SARSr-CoVs and human SARS-CoVs, are  
359 shown in Table 3. Notably, the Ka/Ks ratios for most coding regions of SARSr-BatCoVs,  
360 including ORF8 of SARSr-BatCoVs, were low, supporting purifying selection. In  
361 contrast, many regions of civet SARSr-CoVs and human SARS-CoVs exhibited  
362 relatively high Ka/Ks ratios suggestive of positive selection. Positive selection was  
363 particularly strong at the S (Ka/Ks=3) and ORF3 (Ka/Ks=2) of civet SARSr-CoVs, and  
364 the M (Ka/Ks=2) and ORF8 (Ka/Ks=3.5) of human SARS-CoVs.

365 **Estimation of divergence dates.** Using the uncorrelated relaxed clock model on  
366 ORF1ab, the time of the most recent common ancestor (tMRCA) of all SARSr-CoVs was  
367 estimated to be 1960.1 [highest posterior density regions at 95% (HPD), 1899.1 to  
368 1988.6]. The tMRCA of human and civet SARSr-CoVs was estimated to be 2001.5

369 (HPDs, 1999.1 to 2002.5), approximately 2 years before the SARS epidemic. The  
370 tMRCA of human/civet SARSr-CoVs, SARSr-Rp-BatCoV Rp3/2004, and SARSr-Rs-  
371 BatCoV RsSHC014/2011, Rs3367/2012 and WIV1/2012 was estimated to be 1995.3  
372 (HPDs, 1984.5 to 2001), while that of human/civet SARSr-CoVs, and SARSr-Rf-  
373 BatCoVs, was estimated to be 1990.6 (HPDs, 1973.2 to 1999.6) (Fig. 6).

374 Since some regions in ORF1ab may be involved in recombination (Fig. 5), nsp5,  
375 which was free from recombination, was also used for analysis and showed similar tree  
376 topology. Using the uncorrelated relaxed clock model on nsp5, the time of the most  
377 recent common ancestor (tMRCA) of all SARSr-CoVs was estimated to be 1961.5  
378 [highest posterior density regions at 95% (HPD), 1898.9 to 1991.5]. The tMRCA of  
379 human and civet SARSr-CoVs was estimated to be 2000.7 (HPDs, 1996.7 to 2002.6),  
380 approximately 2 years before the SARS epidemic. The tMRCA of human/civet SARSr-  
381 CoVs, SARSr-Rp-BatCoV Rp3/2004, and SARSr-Rs-BatCoV RsSHC014/2011,  
382 Rs3367/2012 and WIV1/2012 was estimated to be 1996.3 (HPDs, 1985.2 to 2001.7),  
383 while that of human/civet SARSr-CoVs, and SARSr-Rf-BatCoVs, was estimated to be  
384 1989.9 (HPDs, 1969.6 to 2000.3) (Fig. 6) The estimated mean substitution rates of the  
385 ORF1ab and nsp5 data set under the uncorrelated exponentially distributed relaxed clock  
386 model (UCED) were  $2.00 \times 10^{-3}$  and  $1.36 \times 10^{-3}$  substitution per site per year respectively,  
387 which are comparable to other CoVs and RNA viruses (55, 56).

#### 388 **Expression of ORF8 and determination of leader-body junction sequence.**

389 CoVs are characterized by a unique mechanism of discontinuous transcription with the  
390 synthesis of a nested set of subgenomic mRNAs (1, 2). To determine if ORF8 is  
391 expressed in SARSr-Rf-BatCoV and the location of the leader and body TRS used for

392 mRNA synthesis, the leader-body junction sites and flanking sequences of ORF8  
393 subgenomic mRNA were determined. The obtained subgenomic mRNA sequence was  
394 aligned to the leader sequence which confirmed the core sequence of the TRS motifs as  
395 5'-ACGAAC-3' (Fig. 7), as in other SARSr-CoVs. The leader TRS and the ORF8  
396 subgenomic mRNA exactly matched each other. The SARSr-Rf-BatCoV leader was  
397 confirmed as the first 66 nt(s) of the genome.  
398

399 **DISCUSSION**

400 The ORF8 of civet SARSr-CoV is likely to have been acquired from SARSr-Rf-BatCoVs  
401 in greater horseshoe bats (*R. ferrumequinum*) through recombination. In this study, two  
402 SARSr-Rf-BatCoV strains, YNLF\_31C and YNLF\_34C, were identified from greater  
403 horseshoe bats. Although their genomes only possessed 93% nt identities to the genomes  
404 of human/civet SARSr-CoVs, which is lower than the 95% nt identities between  
405 human/civet SARSr-CoV and SARSr-Rs-BatCoVs, Rs3367 and RsSHC014, from  
406 Chinese horseshoe bats in Yunnan, the nsp3 and ORF8 of SARSr-Rf-BatCoV  
407 YNLF\_31C and YNLF\_34C exhibited the highest aa identities among all SARSr-  
408 BatCoVs to that of civet SARSr-CoV SZ3. In particular, their ORF8 demonstrated much  
409 higher aa identities (81.3%) to civet SARSr-CoV SZ3 than SARSr-BatCoVs from other  
410 horseshoe bats (23.2% to 37.3%). Phylogenetic analysis of the ORF8 revealed a distinct  
411 clade formed by human/civet SARSr-CoVs and SARSr-Rf-BatCoVs separate from other  
412 SARSr-BatCoVs. This is in line with a previous report showing that the ORF8 of SARSr-  
413 Rf-BatCoV Rf1 was clustered with human/civet SARSr-CoVs but not SARSr-BatCoV  
414 Rm1 and Rp3 upon phylogenetic analysis, although only one SARSr-Rf-BatCoV strain  
415 was available for analysis (28). Moreover, potential recombination sites were identified  
416 between SARSr-Rf-BatCoVs and SARSr-Rs-BatCoVs around the ORF8 region, leading  
417 to the generation of civet SARSr-CoV SZ3 with the ORF8 acquired from SARSr-Rf-  
418 BatCoVs. Similar to other regions of the genome, the ORF8 of SARSr-Rf-BatCoVs has  
419 been under purifying selection, which supports greater horseshoe bats as a reservoir for  
420 SARSr-Rf-BatCoVs. In contrast, the ORF8 of human SARS-CoVs was under strong  
421 positive selection, which reflects the rapid evolution soon after interspecies jumping.

422 These findings supported that recombination is the key mechanism involved in the  
423 acquisition of ORF8 by the ancestor of civet SARSr-CoVs. In fact, previous studies have  
424 demonstrated frequent recombination events between SARSr-Rs-BatCoV strains from  
425 different bat species of different geographical locations in China (22, 55). Moreover, a  
426 recombination breakpoint at nsp16/S intergenic region was detected between SARSr-Rp-  
427 BatCoV Rp3 from Pearson's horseshoe bats (*Rhinolophus pearsoni*) and SARSr-Rf-  
428 BatCoV Rf1 during the evolution of SARSr-BatCoVs to civet SARSr-CoV (22). On the  
429 other hand, some genomic regions of SARSr-Rf-BatCoV YNLF\_31C and YNLF\_34C,  
430 such as nsp3, RdRp and N, were evolutionarily distinct from two previously reported  
431 SARSr-Rf-BatCoV strains, Rf1 and 273/2005, upon phylogenetic analysis. This suggests  
432 that SARSr-Rf-BatCoVs from different geographical locations in China may have  
433 evolved separately through other recombination events. The present findings offer new  
434 insights into the origin and evolution of SARS-CoV, by showing that the ancestor of civet  
435 SARSr-CoV is a likely recombinant virus with ORF8 originated from SARSr-Rf-  
436 BatCoVs in greater horseshoe bats and other genome regions from different horseshoe  
437 bats.

438 Although SARSr-Rs-BatCoV Rs3367 and RsSHC014 represented the closest bat  
439 CoVs to SARS-CoV in terms of genome identity, they were unlikely the immediate  
440 ancestor of civet SARSr-CoVs. Previous molecular-dating studies estimated that the time  
441 of divergence between human/civet and bat SARSr-CoVs ranged from 4 to 17 years  
442 before the SARS epidemic (22, 55, 57). SARSr-CoVs were also shown to be a newly  
443 emerged subgroup of *Betacoronavirus*, with the median date of their MRCA estimated to  
444 be from 1961 to 1982 (55, 57). The present results are in line with such estimations, with

445 the tMRCA between human/civet and closest bat strains estimated to be approximately  
446 1995 (8 years before the SARS epidemic) and that among all SARSr-CoVs  
447 approximately 1960 using ORF1ab. Similar results were also obtained when using nsp5  
448 region which was recombination-free. Moreover, we demonstrated that SARSs-Rf-  
449 BatCoV YNLF\_31C and YNLF\_34C only diverged from civet/human SARSr-CoVs at  
450 approximately 1990. This is in contrast to previous studies that showed SARSr-Rp-  
451 BatCoV Rp3 as the only recently diverged strain (55, 57). Together with the evidence on  
452 the acquisition of ORF8, it is likely that civet SARSr-CoV is originated from  
453 recombination between SARS-Rs-BatCoVs and SARS-Rf-BatCoVs from different  
454 horseshoe bat species within several years before the SARS epidemic.

455       The overlapping habitat and geographical distribution of different horseshoe bats  
456 may have fostered recombination between different SARSr-BatCoVs and emergence of  
457 SARS-CoV. Chinese horseshoe bats are widely distributed throughout China including  
458 Yunnan, Guangdong and Hong Kong. While greater horseshoe bats are also widely  
459 distributed across different provinces in China including Yunnan, they are not found in  
460 Guangdong (58). The two bat species shared similar diet and habits such as the ability to  
461 roost in man-made structures, suggesting that they may co-habitat in similar  
462 environments in Yunnan, the province with the highest biodiversity in China. In fact,  
463 SARSr-Rf-BatCoV YNLF\_31C and YNLF\_34C, and SARSr-Rs-BatCoV Rs3367 and  
464 RsSHC014 were detected in Lufeng and Kunming of the Yunnan province respectively,  
465 which were only ~80 km apart and within the migration distances of horseshoe bats (Fig.  
466 1) (22, 59, 60). Since greater horseshoe bats are not found in Guangdong, recombination  
467 between SARSr-Rf-BatCoVs and SARS-Rs-BatCoVs with the generation of the ancestor



468 of civet SARSr-CoVs may have occurred in yet unidentified bats in Yunnan or nearby  
469 provinces, which were then transported to wildlife markets in Guangdong and infected  
470 civets. Alternatively, recombination may have occurred in civets or other animals within  
471 wildlife farms or markets where many different wild animal species are often housed  
472 together (61). A possible scenario is that the animals were co-infected with SARSr-Rf-  
473 BatCoVs and SARSr-Rs-BatCoVs from different horseshoe bats, followed by  
474 recombination events. More extensive surveillance in bats from Yunnan and neighboring  
475 provinces, as well as wildlife markets in Guangdong may reveal the immediate ancestor  
476 of civet SARSr-CoVs.

477       The ORF8 region, unique to SARSr-CoVs, is prone to mutations or deletions  
478 during interspecies transmission. One of the most striking genomic changes observed in  
479 SARS-CoV soon after its zoonotic transmission to humans was the acquisition of a  
480 characteristic 29-nt deletion which splits ORF8 into two ORFs, ORF8a and ORF8b (25,  
481 62). While SARS-CoVs isolated from the later human cases of the epidemic contained  
482 this 29-nt deletion, isolates from civets and some early human cases possessed a single  
483 continuous ORF8 (25, 63). Besides, some early human strains and a farmed civet strain  
484 from Hubei possessed an alternative 82-nt deletion in ORF8 (63). On the other hand, four  
485 late human isolates possessed a 415-nt deletion, resulting in the loss of the entire ORF8  
486 (63). Although studies using reverse genetics showed that the ORF8 is not essential for  
487 virus replication *in vitro* and *in vivo* (64, 65), the full-length 8ab protein is a functional  
488 protein that is delivered by a cleavable signal sequence to the lumen of the endoplasmic  
489 reticulum where it becomes N-glycosylated (62). Different subcellular localizations and  
490 functions have also been reported for 8ab, 8a and 8b proteins (66-69). Inside the

491 endoplasmic reticulum, 8ab activates the ATF6 branch of unfolded-protein response (70).  
492 The 8a protein enhances SARS-CoV replication and induces caspase-dependent apoptosis  
493 through a mitochondria-dependent pathway (66). Moreover, antibodies against 8a protein  
494 have been detected in sera of SARS patients (66). The 8b protein down-regulates the  
495 expression of the E protein, which supported a modulatory role in viral replication (68).  
496 Moreover, overexpression of the 8b protein induces DNA synthesis (67). The 8b and 8ab  
497 proteins also play a role in the host ubiquitin-proteasome system (71). In this study, the  
498 expression of ORF8 subgenomic mRNA in SARSr-Rf-BatCoV YNLF\_31C suggested  
499 that this protein may also be functional in SARSr-BatCoVs. Moreover, the high Ka/Ks  
500 ratio among human SARS-CoVs compared to SARSr-BatCoVs supported that ORF8 is  
501 subject to rapid evolution under strong positive selection during animal-to-human  
502 transmission. Further studies may help understand the importance of ORF8 evolution for  
503 interspecies transmission of SARSr-CoVs.

504 Besides SARSr-BatCoVs, diverse *alphacoronaviruses* and *betacoronaviruses*,  
505 including potentially novel CoVs, with potential interspecies transmission events were  
506 identified in this study. Bats are known important reservoirs of lineage B, C and D  
507 *betacoronaviruses*, while rodents are likely the reservoir of lineage A *betacoronaviruses*  
508 (30). Nine samples belonging to lineage D *betacoronaviruses* were detected in  
509 Leschenault's rosettes (*R. leschenaulti*), a known reservoir of Ro-BatCoV HKU9 (24).  
510 However, the partial RdRp sequences only possessed 75-79% nt sequences to the latter,  
511 suggesting that they may represent either novel CoV species or novel genotype of Ro-  
512 BatCoV HKU9. As for *alphacoronaviruses*, 24 samples from Daubenton's bats (*M.*  
513 *daubentonii*) contained viruses most closely related to My-BatCoV HKU6 with 78-99%

514 nt identities in the partial RdRp region, which may represent My-BatCoV HKU6 or  
515 related viruses previously reported in the same bat species (38). Six samples contained  
516 *alphacoronaviruses* most closely related to Rh-BatCoV HKU2. However, four samples  
517 (YNXY\_7C, YNXY\_10C, YNXY\_45 and YNXY\_50C) from Daubenton's bats  
518 possessed partial RdRp sequences of only 80-80% nt identities to that of Rh-BatCoV  
519 HKU2, suggesting that they may represent novel CoVs. Although the other two samples  
520 (MJ\_27C and MJ\_69C) possessed RdRp sequences with 92-93% identities to that of Rh-  
521 BatCoV HKU2, they were detected from Daubenton's bats and lesser brown horseshoe  
522 bats (*R. steno*) instead of Chinese horseshoe bats (*R. sinicus*) previously reported to  
523 carry Rh-BatCoV HKU2 (34). This may suggest interspecies transmission of Rh-BatCoV  
524 HKU2 among different bat species. Two samples from Pomona roundleaf bats  
525 (*Hipposideros Pomona*) contained *alphacoronaviruses* most closely related to Hi-  
526 BatCoV HKU10. However, the partial RdRp sequences only possessed 81-87% nt  
527 identity to the latter. We have previously described recent interspecies transmission of  
528 BatCoV HKU10 between Leschenault's rousettes (*R. leschenaulti*) and Pomona  
529 roundleaf bats, two very different bats belonging to different families, through rapid  
530 evolution of the S protein (72). Further studies are warranted to determine if the two  
531 samples from Pomona roundleaf bats contained potentially novel CoVs closely related to  
532 BatCoV HKU10 or variants of BatCoV HKU10 due to interspecies transmission.

533 **ACKNOWLEDGEMENTS**

534 We thank Dr. Wing-Man Ko, Secretary for Food and Health Bureau; and Dr. Constance Hon-  
535 Yee Chan, Director of Health, for facilitation and support. We are grateful to the generous  
536 support of Mrs. Carol Yu, Professor Richard Yu, Mr. Hui Hoy and Mr. Hui Ming in the  
537 genomic sequencing platform.

538 This work is partly supported by Health and Medical Research Fund of the Food and  
539 Health Bureau of HKSAR (13121102); the Theme-Based Research Scheme and Research Grant  
540 Council Grant, University Grant Council; Croucher Senior Medical Research Fellowships,  
541 Committee for Research and Conference Grant, Strategic Research Theme Fund, University  
542 Development Fund and Special Research Achievement Award, The University of Hong Kong;  
543 and Consultancy Service for Enhancing Laboratory Surveillance of Emerging Infectious  
544 Disease for the HKSAR Department of Health.

545

## 546 REFERENCES

- 547 1. **Brian DA, Baric RS.** 2005. Coronavirus genome structure and replication. *Curr Top*  
548 *Microbiol Immunol* **287**:1-30.
- 549 2. **Lai MM, Cavanagh D.** 1997. The molecular biology of coronaviruses. *Adv Virus Res*  
550 **48**:1-100.
- 551 3. **de Groot RJ, Baker SC, Baric R, Enjuanes L, Gorbalenya A, Holmes KV, Perlman**  
552 **S, Poon L, Rottier PJ, Talbot PJ, Woo PC, Ziebuhr J.** 2011. *Coronaviridae*. In:  
553 *Virus Taxonomy, Classification and Nomenclature of Viruses, Ninth Report of the*  
554 *International Committee on Taxonomy of Viruses, International Union of*  
555 *Microbiological Societies, Virology Division, King AMQ, Adams MJ, Carstens EB,*  
556 *Lefkowitz EJ, eds. Elsevier Academic Press, pp. 806-828.*
- 557 4. **Woo PC, Lau SK, Lam CS, Lau CC, Tsang AK, Lau JH, Bai R, Teng JL, Tsang**  
558 **CC, Wang M, Zheng BJ, Chan KH, Yuen KY.** 2012. Discovery of seven novel  
559 mammalian and avian coronaviruses in *Deltacoronavirus* supports bat coronaviruses as  
560 the gene source of *Alphacoronavirus* and *Betacoronavirus* and avian coronaviruses as  
561 the gene source of *Gammacoronavirus* and *Deltacoronavirus*. *J Virol* **86**:3995-4008.
- 562 5. **Woo PC, Wang M, Lau SK, Xu H, Poon RW, Guo R, Wong BH, Gao K, Tsoi HW,**  
563 **Huang Y, Li KS, Lam CS, Chan KH, Zheng BJ, Yuen KY.** 2006. Comparative  
564 analysis of 12 genomes of three novel group 2c and group 2d coronaviruses reveals  
565 unique group and subgroup features. *J Virol* **81**:1574-1585.
- 566 6. **Gorbalenya AE, Snijder EJ, Spaan WJ.** 2004 Severe acute respiratory syndrome  
567 coronavirus phylogeny: towards consensus. *J Virol* **78**:7863-7866.

- 568 7. **Drosten C, Günther S, Preiser W, van der Werf S, Brodt HR, Becker S, Rabenau**  
569 **H, Panning M, Kolesnikova L, Fouchier RA, Berger A, Burguière AM, Cinatl J,**  
570 **Eickmann M, Escriou N, Grywna K, Kramme S, Manuguerra JC, Müller S,**  
571 **Rickerts V, Stürmer M, Vieth S, Klenk HD, Osterhaus AD, Schmitz H, Doerr HW.**  
572 2003. Identification of a Novel Coronavirus in Patients with Severe Acute Respiratory  
573 Syndrome. *N Engl J Med* **348**:1967-1976.
- 574 8. **Fouchier RA, Hartwig NG, Bestebroer TM, Niemeyer B, de Jong JC, Simon JH,**  
575 **Osterhaus AD.** 2004. A previously undescribed coronavirus associated with respiratory  
576 disease in humans. *Proc Natl Acad Sci USA* **101**:6212-6216.
- 577 9. **Ksiazek TG, Erdman D, Goldsmith CS, Zaki SR, Peret T, Emery S, Tong S,**  
578 **Urbani C, Comer JA, Lim W, Rollin PE, Dowell SF, Ling AE, Humphrey CD,**  
579 **Shieh WJ, Guarner J, Paddock CD, Rota P, Fields B, DeRisi J, Yang JY, Cox N,**  
580 **Hughes JM, LeDuc JW, Bellini WJ, Anderson LJ; SARS Working Group.** 2003. A  
581 novel coronavirus associated with severe acute respiratory syndrome. *N Engl J Med*  
582 **348**:1953-1966.
- 583 10. **Peiris JS, Lai ST, Poon LL, Guan Y, Yam LY, Lim W, Nicholls J, Yee WK, Yan**  
584 **WW, Cheung MT, Cheng VC, Chan KH, Tsang DN, Yung RW, Ng TK, Yuen KY.**  
585 2003. Coronavirus as a possible cause of severe acute respiratory syndrome. *Lancet*  
586 **361**:1319-1325.
- 587 11. **van der Hoek L, Pyrc K, Jebbink MF, Vermeulen-Oost W, Berkhout RJ, Wolthers**  
588 **KC, Wertheim-van Dillen PM, Kaandorp J, Spaargaren J, Berkhout B.** 2004.  
589 Identification of a new human coronavirus. *Nat Med* **10**:368-373.

- 590 12. **Woo PC, Lau SK, Chu CM, Chan KH, Tsoi HW, Huang Y, Wong BH, Poon RW,**  
591 **Cai JJ., Luk WK, Poon LL, Wong SS, Guan Y, Peiris JS, Yuen KY.** 2005.  
592 Characterization and complete genome sequence of a novel coronavirus, coronavirus  
593 HKU1, from patients with pneumonia. *J Virol* **79**:884-895.
- 594 13. **Woo PC, Lau SK, Tsoi HW, Huang Y, Poon RW, Chu CM, Lee RA, Luk WK,**  
595 **Wong GK, Wong BH, Cheng VC, Tang BS, Wu AK, Yung RW, Chen H, Guan Y,**  
596 **Chan KH, Yuen KY.** 2005. Clinical and molecular epidemiological features of  
597 coronavirus HKU1-associated community-acquired pneumonia. *J Infect Dis* **192**:1898-  
598 1907.
- 599 14. **Zaki AM, van Boheemen S, Bestebroer TM, Osterhaus AD, Fouchier RA.** 2012.  
600 Isolation of a novel coronavirus from a man with pneumonia in Saudi Arabia. *N Engl J*  
601 *Med* **367**:1814-1820.
- 602 15. **van Boheemen S, de Graaf M, Lauber C, Bestebroer TM, Raj VS, Zaki AM,**  
603 **Osterhaus AD, Haagmans BL, Gorbalenya AE, Snijder EJ, Fouchier RA.** 2012.  
604 Genomic characterization of a newly discovered coronavirus associated with acute  
605 respiratory distress syndrome in humans. *MBio* **3**(6).
- 606 16. **de Groot RJ, Baker SC, Baric RS, Brown CS, Drosten C, Enjuanes L, Fouchier RA,**  
607 **Galiano M, Gorbalenya AE, Memish ZA, Perlman S, Poon LL, Snijder EJ,**  
608 **Stephens GM, Woo PC, Zaki AM, Zambon M, Ziebuhr J.** 2013. Middle East  
609 respiratory syndrome coronavirus (MERS-CoV): announcement of the Coronavirus  
610 Study Group. *J Virol* **87**:7790-7792.

- 611 17. **Herrewegh AA, Smeenk I, Horzinek MC, Rottier PJ, de Groot RJ.** 1998. Feline  
612 coronavirus type II strains 79-1683 and 79-1146 originate from a double recombination  
613 between feline coronavirus type I and canine coronavirus. *J Virol* **72**:4508-4514.
- 614 18. **Woo PC, Lau SK, Yip CC, Huang Y, Tsoi HW, Chan KH, Yuen KY.** 2006.  
615 Comparative analysis of 22 coronavirus HKU1 genomes reveals a novel genotype and  
616 evidence of natural recombination in coronavirus HKU1. *J Virol* **80**:7136-7145.
- 617 19. **Keck JG, Matsushima GK, Makino S, Fleming JO, Vannier DM, Stohlman SA,**  
618 **Lai MM.** 1988. In vivo RNA-RNA recombination of coronavirus in mouse brain. *J*  
619 *Virol* **62**:1810-1813.
- 620 20. **Kottier SA, Cavanagh D, Britton P.** 1995. Experimental evidence of recombination in  
621 coronavirus infectious bronchitis virus. *Virology* **213**:569-580.
- 622 21. **Lau SK, Woo PC, Yip CC, Fan RY, Huang Y, Wang M, Guo R, Lam CS, Tsang**  
623 **AK, Lai KK, Chan KH, Che XY, Zheng BJ, Yuen KY.** 2012. Isolation and  
624 characterization of a novel Betacoronavirus subgroup A coronavirus, rabbit coronavirus  
625 HKU14, from domestic rabbits. *J Virol* **86**:5481-5496.
- 626 22. **Lau SK, Li KS, Huang Y, Shek CT, Tse H, Wang M, Choi GK, Xu H, Lam CS,**  
627 **Guo R, Chan KH, Zheng BJ, Woo PC, Yuen KY.** 2010. Ecoepidemiology and  
628 complete genome comparison of different strains of severe acute respiratory syndrome-  
629 related Rhinolophus bat coronavirus in China reveal bats as a reservoir for acute, self-  
630 limiting infection that allows recombination events. *J Virol* **84**:2808-2819.
- 631 23. **Lau SK, Lee P, Tsang AK, Yip CC, Tse H, Lee RA, So LY, Lau YL, Chan KH,**  
632 **Woo PC, Yuen KY.** 2011. Molecular epidemiology of human coronavirus OC43



- 633 reveals evolution of different genotypes over time and recent emergence of a novel  
634 genotype due to natural recombination. *J Virol* **85**:11325-11337.
- 635 24. **Lau SK, Poon RW, Wong BH, Wang M, Huang Y, Xu H, Guo R, Li KS, Gao K,**  
636 **Chan KH, Zheng BJ, Woo PC, Yuen KY.** 2010. Coexistence of different genotypes in  
637 the same bat and serological characterization of Rousettus bat coronavirus HKU9  
638 belonging to a novel Betacoronavirus subgroup. *J Virol* **84**:11385-11394.
- 639 25. **Guan Y, Zheng BJ, He YQ, Liu XL, Zhuang ZX, Cheung CL, Luo SW, Li PH,**  
640 **Zhang LJ, Guan YJ, Butt KM, Wong KL, Chan KW, Lim W, Shortridge KF,**  
641 **Yuen KY, Peiris JS, Poon LL.** 2003. Isolation and characterization of viruses related  
642 to the SARS coronavirus from animals in southern China. *Science* **302**:276-278.
- 643 26. **Yang ZY, Werner HC, Kong WP, Leung K, Traggiai E, Lanzavecchia A, Nabel GJ.**  
644 2005. Evasion of antibody neutralization in emerging severe acute respiratory syndrome  
645 coronaviruses. *Proc Natl Acad Sci USA* **102**:797-801.
- 646 27. **Lau SK, Woo PC, Li KS, Huang Y, Tsoi HW, Wong BH, Wong SS, Leung SY,**  
647 **Chan KH, Yuen KY.** 2005. Severe acute respiratory syndrome coronavirus-like virus  
648 in Chinese horseshoe bats. *Proc. Natl. Acad. Sci. USA* **102**:14040-14045.
- 649 28. **Li W, Shi Z, Yu M, Ren W, Smith C, Epstein JH, Wang H, Crameri G, Hu Z,**  
650 **Zhang H, Zhang J, McEachern J, Field H, Daszak P, Eaton BT, Zhang S, Wang**  
651 **LF.** 2005. Bats are natural reservoirs of SARS-like coronaviruses. *Science* **310**:676-679.
- 652 29. **Woo PC, Lau SK, Li KS, Poon RW, Wong BH, Tsoi HW, Yip BC, Huang Y, Chan**  
653 **KH, Yuen KY.** 2006. Molecular diversity of coronaviruses in bats. *Virology* **351**:180-  
654 187.

- 655 30. **Lau SK, Woo PC, Li KS, Tsang AK, Fan RY, Luk HK, Cai JP, Chan KH, Zheng**  
656 **BJ, Wang M, Yuen KY.** 2015. Discovery of a novel coronavirus, China Rattus  
657 coronavirus HKU24, from Norway rats supports murine origin of Betacoronavirus 1  
658 with implications on the ancestor of *Betacoronavirus* lineage A. J Virol **89**:3076-3092.
- 659 31. **Brandão PE, Scheffer K, Villarreal LY, Achkar S, Oliveira Rde N, Fahl Wde O,**  
660 **Castilho JG, Kotait I, Richtzenhain LJ.** 2008. A coronavirus detected in the vampire  
661 bat *Desmodus rotundus*. Braz J Infect Dis **12**:466-468.
- 662 32. **Dominguez SR, O'Shea TJ, Oko LM, Holmes KV.** 2007. Detection of group 1  
663 coronaviruses in bats in North America. Emerg Infect Dis **13**:1295-1300.
- 664 33. **Gloza-Rausch F, Ipsen A, Seebens A, Gottsche M, Panning M, Felix Drexler J,**  
665 **Petersen N, Annan A, Grywna K, Muller M, Pfefferle S, Drosten C.** 2008. Detection  
666 and prevalence patterns of group I coronaviruses in bats, northern Germany. Emerg  
667 Infect Dis **14**:626-631.
- 668 34. **Lau SK, Woo PC, Li KS, Huang Y, Wang M, Lam CS, Xu H, Guo R, Chan KH,**  
669 **Zheng BJ, Yuen KY.** 2007. Complete genome sequence of bat coronavirus HKU2  
670 from Chinese horseshoe bats revealed a much smaller spike gene with a different  
671 evolutionary lineage from the rest of the genome. Virology **367**:428-439.
- 672 35. **Pfefferle S, Oppong S, Drexler JF, Gloza-Rausch F, Ipsen A, Seebens A, Muller**  
673 **MA, Annan A, Vallo P, Adu-Sarkodie Y, Kruppa TF, Drosten C.** 2009. Distant  
674 relatives of severe acute respiratory syndrome coronavirus and close relatives of human  
675 coronavirus 229E in bats, Ghana. Emerg Infect Dis **15**:1377-1384.

- 676 36. **Poon LL, Chu DK, Chan KH, Wong OK, Ellis TM, Leung YH, Lau SK, Woo PC,**  
677 **Suen KY, Yuen KY, Guan Y, Peiris JS.** 2005. Identification of a novel coronavirus in  
678 bats. *J Virol* **79**:2001-2009.
- 679 37. **Tang XC, Zhang JX, Zhang SY, Wang P, Fan XH, Li LF, Li G, Dong BQ, Liu W,**  
680 **Cheung CL, Xu KM, Song WJ, Vijaykrishna D, Poon LL, Peiris JS, Smith GJ,**  
681 **Chen H, Guan Y.** 2006. Prevalence and genetic diversity of coronaviruses in bats from  
682 China. *J Virol* **80**:7481-7490.
- 683 38. **He B, Zhang Y, Xu L, Yang W, Yang F, Feng Y, Xia L, Zhou J, Zhen W, Feng Y,**  
684 **Guo H, Zhang H, Tu C.** 2014. Identification of diverse alphacoronaviruses and  
685 genomic characterization of a novel severe acute respiratory syndrome-like coronavirus  
686 from bats in China. *J Virol* **88**:7070-7082.
- 687 39. **Reusken CB, Haagmans BL, Muller MA, Gutierrez C, Godeke GJ, Meyer B, Muth**  
688 **D, Raj VS, Smits-De Vries L, Corman VM, Drexler JF, Smits SL, El Tahir YE, De**  
689 **Sousa R, van Beek J, Nowotny N, van Maanen K, Hidalgo-Hermoso E, Bosch BJ,**  
690 **Rottier P, Osterhaus A, Gortazar-Schmidt C, Drosten C, Koopmans MP.** 2013.  
691 Middle East respiratory syndrome coronavirus neutralising serum antibodies in  
692 dromedary camels: a comparative serological study. *Lancet Infect Dis* **13**:859-866.
- 693 40. **Haagmans BL, Al Dhahiry SH, Reusken CB, Raj VS, Galiano M, Myers R, Godeke**  
694 **GJ, Jonges M, Farag E, Diab A, Ghobashy H, Alhajri F, Al-Thani M, Al-Marri SA,**  
695 **Al Romaihi HE, Al Khal A, Bermingham A, Osterhaus AD, AlHajri MM,**  
696 **Koopmans MP.** 2014. Middle East respiratory syndrome coronavirus in dromedary  
697 camels: an outbreak investigation. *Lancet Infect Dis* **14**:140-145.

- 698 41. **Chan JF, Lau SK, To KK, Cheng VC, Woo PC, Yuen KY.** 2015. Middle East  
699 Respiratory Syndrome Coronavirus: Another Zoonotic Betacoronavirus Causing SARS-  
700 Like Disease. *Clin Microbiol Rev* **28**:465-522.
- 701 42. **Ge XY, Li JL, Yang XL, Chmura AA, Zhu G, Epstein JH, Mazet JK, Hu B, Zhang**  
702 **W, Peng C, Zhang YJ, Luo CM, Tan B, Wang N, Zhu Y, Crameri G, Zhang SY,**  
703 **Wang LF, Daszak P, Shi ZL.** 2013. Isolation and characterization of a bat SARS-like  
704 coronavirus that uses the ACE2 receptor. *Nature* **503**:535-538.
- 705 43. **Yang L, Wu Z, Ren X, Yang F, He G, Zhang J, Dong J, Sun L, Zhu Y, Du J, Zhang**  
706 **S, Jin Q.** 2013. Novel SARS-like betacoronaviruses in bats, China, 2011. *Emerg Infect*  
707 *Dis* **19**:989-991.
- 708 44. **Tong S, Conrardy C, Ruone S, Kuzmin IV, Guo X, Tao Y, Niezgoda M, Haynes L,**  
709 **Agwand B, Breiman RF, Anderson LJ, Rupprecht CE.** 2009. Detection of novel  
710 SARS-like and other coronaviruses in bats from Kenya. *Emerg Infect Dis* **15**:482-485.
- 711 45. **Quan PL, Firth C, Street C, Henriquez JA, Petrosov A, Tashmukhamedova A,**  
712 **Hutchison SK, Egholm M, Osinubi MO, Niezgoda M, Ogunkoya AB, Briese T,**  
713 **Rupprecht CE, Lipkin WI.** 2010. Identification of a severe acute respiratory syndrome  
714 coronavirus-like virus in a leaf-nosed bat in Nigeria. *MBio* **1**(4).
- 715 46. **Yob JM, Field H, Rashdi AM, Morrissy C, van der Heide B, Rota P, bin Adzhar A,**  
716 **White J, Daniels P, Jamaluddin A, Ksiazek T.** 2001. Nipah virus infection in bats  
717 (order *Chiroptera*) in peninsular Malaysia. *Emerg Infect Dis* **7**:439-441.
- 718 47. **Lau SK, Li KS, Tsang AK, Lam CS, Ahmed S, Chen H, Chan KH, Woo PC, Yuen**  
719 **KY.** 2013. Genetic characterization of *Betacoronavirus* lineage C viruses in bats reveals  
720 marked sequence divergence in the spike protein of *Pipistrellus* bat coronavirus HKU5

- 721 in *Japanese pipistrelle*: implications for the origin of the novel Middle East respiratory  
722 syndrome coronavirus. J Virol **87**:8638-8650.
- 723 48. **Huang Y, Lau SK, Woo PC, Yuen KY.** 2008. CoVDB: a comprehensive database for  
724 comparative analysis of coronavirus genes and genomes. Nucleic Acids Res **36**:D504-  
725 D511.
- 726 49. **Lole KS, Bollinger RC, Paranjape RS, Gadkari D, Kulkarni SS, Novak NG,**  
727 **Ingersoll R, Sheppard HW, Ray SC.** 1999. Full-length human immunodeficiency  
728 virus type 1 genomes from subtype C-infected seroconverters in India, with evidence of  
729 intersubtype recombination. J Virol **73**:152-160.
- 730 50. **Drummond AJ, Rambaut A.** 2007. BEAST: Bayesian evolutionary analysis by  
731 sampling trees. BMC Evol Biol **7**:214.
- 732 51. **Pyrce K, Jebbink MF, Berkhout B, van der Hoek L.** 2004. Genome structure and  
733 transcriptional regulation of human coronavirus NL63. Virol J **1**:7.
- 734 52. **Ren W, Li W, Yu M, Hao P, Zhang Y, Zhou P, Zhang S, Zhao G, Zhong Y, Wang**  
735 **S, Wang LF, Shi Z.** 2006. Full-length genome sequences of two SARS-like  
736 coronaviruses in horseshoe bats and genetic variation analysis. J Gen Virol **87**:3355-  
737 3359.
- 738 53. **Song HD, Tu CC, Zhang GW, Wang SY, Zheng K, Lei LC, Chen QX, Gao YW,**  
739 **Zhou HQ, Xiang H, Zheng HJ, Chern SW, Cheng F, Pan CM, Xuan H, Chen SJ,**  
740 **Luo HM, Zhou DH, Liu YF, He JF, Qin PZ, Li LH, Ren YQ, Liang WJ, Yu YD,**  
741 **Anderson L, Wang M, Xu RH, Wu XW, Zheng HY, Chen JD, Liang G, Gao Y,**  
742 **Liao M, Fang L, Jiang LY, Li H, Chen F, Di B, He LJ, Lin JY, Tong S, Kong X, Du**  
743 **L, Hao P, Tang H, Bernini A, Yu XJ, Spiga O, Guo ZM, Pan HY, He WZ,**

- 744 **Manuguerra JC, Fontanet A, Danchin A, Niccolai N, Li YX, Wu CI, Zhao GP.**  
745 2005. Cross-host evolution of severe acute respiratory syndrome coronavirus in palm  
746 civet and human. *Proc Natl Acad Sci USA* **102**:2430-2435.
- 747 54. **Li W, Zhang C, Sui J, Kuhn JH, Moore MJ, Luo S, Wong SK, Huang IC, Xu K,**  
748 **Vasilieva N, Murakami A, He Y, Marasco WA, Guan Y, Choe H, Farzan M.** 2005.  
749 Receptor and viral determinants of SARS-coronavirus adaptation to human ACE2.  
750 *EMBO J* **24**:1634-1643.
- 751 55. **Hon CC, Lam TY, Shi ZL, Drummond AJ, Yip CW, Zeng F, Lam PY, Leung FC.**  
752 2008. Evidence of the recombinant origin of a bat severe acute respiratory syndrome  
753 (SARS)-like coronavirus and its implications on the direct ancestor of SARS  
754 coronavirus. *J Virol* **82**:1819-1826.
- 755 56. **Jenkins GM, Rambaut A, Pybus OG, Holmes EC.** 2002. Rates of molecular  
756 evolution in RNA viruses: a quantitative phylogenetic analysis. *J Mol Evol* **54**:156-165.
- 757 57. **Vijaykrishna D, Smith GJ, Zhang JX, Peiris JS, Chen H, Guan Y.** 2007.  
758 Evolutionary insights into the ecology of coronaviruses. *J Virol* **81**:4012-4020.
- 759 58. **Flanders J, Wei L, Rossiter SJ, Zhang S.** 2011. Identifying the effects of the greater  
760 horseshoe bat, *Rhinolophus ferrumequinum*, in East Asia using ecological niche  
761 modelling and phylogenetic analyses. *J Biogeogr* **38**:439-452
- 762 59. **Neuweiler G.** 2000. *In* The Biology of Bat, p.266. Oxford University Press, New York.
- 763 60. **Nowak RM, Paradiso JL.** 1983. *In* Walker's mammals of the world, p.230. The Johns  
764 Hopkins University Press, Baltimore and London.

- 765 61. **Woo PC, Lau SK, Yuen KY.** 2006. Infectious diseases emerging from Chinese wet-  
766 markets: zoonotic origins of severe respiratory viral infections. *Curr Opin Infect Dis*  
767 **19**:401-407.
- 768 62. **Oostra M, de Haan CA, Rottier PJ.** 2007. The 29-nucleotide deletion present in  
769 human but not in animal severe acute respiratory syndrome coronaviruses disrupts the  
770 functional expression of open reading frame 8. *J Virol* **81**:13876-13888.
- 771 63. **Chinese SARS Molecular Epidemiology Consortium.** 2004. Molecular evolution of  
772 the SARS coronavirus during the course of the SARS epidemic in China. *Science*  
773 **303**:1666-1669.
- 774 64. **Yount B, Roberts RS, Sims AC, Deming D, Frieman MB, Sparks J, Denison MR,**  
775 **Davis N, Baric RS.** 2005. Severe acute respiratory syndrome coronavirus group-  
776 specific open reading frames encode nonessential functions for replication in cell  
777 cultures and mice. *J Virol* **79**:14909-14922.
- 778 65. **Dediego ML, Pewe L, Alvarez E, Rejas MT, Perlman S, Enjuanes L.** 2008.  
779 Pathogenicity of severe acute respiratory coronavirus deletion mutants in hACE-2  
780 transgenic mice. *Virology* **376**:379-389.
- 781 66. **Chen CY, Ping YH, Lee HC, Chen KH, Lee YM, Chan YJ, Lien TC, Jap TS, Lin**  
782 **CH, Kao LS, Chen YM.** 2007. Open reading frame 8a of the human severe acute  
783 respiratory syndrome coronavirus not only promotes viral replication but also induces  
784 apoptosis. *J Infect Dis* **196**:405-415.
- 785 67. **Law PY, Liu YM, Geng H, Kwan KH, Waye MM, Ho YY.** 2006. Expression and  
786 functional characterization of the putative protein 8b of the severe acute respiratory  
787 syndrome-associated coronavirus. *FEBS Lett* **580**:3643-3648.

- 788 68. **Keng CT, Choi YW, Welkers MR, Chan DZ, Shen S, Gee Lim S, Hong W, Tan YJ.**  
789 2006. The human severe acute respiratory syndrome coronavirus (SARS-CoV) 8b  
790 protein is distinct from its counterpart in animal SARS-CoV and down-regulates the  
791 expression of the envelope protein in infected cells. *Virology* **354**:132-142.
- 792 69. **Liu DX, Fung TS, Chong KK, Shukla A, Hilgenfeld R.** 2014. Accessory proteins of  
793 SARS-CoV and other coronaviruses. *Antiviral Res* **109**:97-109.
- 794 70. **Sung SC, Chao CY, Jeng KS, Yang JY, Lai MM.** 2009. The 8ab protein of SARS-  
795 CoV is a luminal ER membrane-associated protein and induces the activation of ATF6.  
796 *Virology* **387**:402-413.
- 797 71. **Le TM, Wong HH, Tay FP, Fang S, Keng CT, Tan YJ, Liu DX.** 2007. Expression,  
798 post-translational modification and biochemical characterization of proteins encoded by  
799 subgenomic mRNA8 of the severe acute respiratory syndrome coronavirus. *FEBS J*  
800 **274**:4211-4222.
- 801 72. **Lau SK, Li KS, Tsang AK, Shek CT, Wang M, Choi GK, Guo R, Wong BH, Poon**  
802 **RW, Lam CS, Wang SY, Fan RY, Chan KH, Zheng BJ, Woo PC, Yuen KY.** 2012.  
803 Recent transmission of a novel alphacoronavirus, bat coronavirus HKU10, from  
804 Leschenault's rousettes to pomona leaf-nosed bats: first evidence of interspecies  
805 transmission of coronavirus between bats of different suborders. *J Virol* **86**:11906-  
806 11918.  
807



808 **LEGENDS TO FIGURES**

809 **FIG 1** Map showing five locations of bat sampling in four autonomous prefectures (AP) in  
810 Yunnan Province, China. Sampling locations in Yunnan are in red. The location of SARSr-Rs-  
811 BatCoV strains, Rs3367 and RsSHC014, detected in a previous study (42) is in blue.

812 **FIG 2** Phylogenetic analysis of the nt sequences of the 267-nt fragment of RdRp of the 46  
813 positive samples identified in bats in Yunnan in this study. The tree was constructed by  
814 maximum likelihood method with the model GTR+G. Bootstrap values were calculated from  
815 1000 trees and only values >700 are shown and given at nodes. The scale bar indicates 5 nt  
816 substitutions per site. The two SARSr-Rf-BatCoV strains YNLF\_31C and YNLF\_34C are in  
817 red. The potentially novel bat CoVs are in purple. AntelopeCoV, sable antelope coronavirus  
818 (EF424621); BatCoV CDPHE15/USA/2006, Bat coronavirus CDPHE15/USA/2006  
819 (NC\_022103.1); BatCoV/SC2013, Betacoronavirus/SC2013 (KJ473821.1); Erinaceus  
820 CoV/VMC/DEU/2012, Betacoronavirus Erinaceus/VMC/DEU/2012 (NC\_022643); BCoV, bovi  
821 ne coronavirus (NC\_003045); BdHKU22, bottlenose dolphin coronavirus HKU22 (KF793826);  
822 BuCoV HKU11, bulbul coronavirus HKU11 (FJ376619); BWCoV SW1, beluga whale  
823 coronavirus SW1 (NC\_010646); CCoV, Canine coronavirus strain CCoV/NTU336/F/2008  
824 (GQ477367.1); CCRCoV, Canine respiratory coronavirus strain K37 (JX860640.1); CmCoV  
825 HKU21, common moorhen coronavirus HKU21 (NC\_016996); CoV Neoromicia/PML-  
826 PHE1/RSA/2011, coronavirus Neoromicia/PML-PHE1/RSA/2011 (KC869678); DcCoV  
827 HKU23, dromedary camel coronavirus HKU23 (KF906251); ECoV, equine coronavirus  
828 (NC\_010327); FIPV, feline infectious peritonitis virus (AY994055); GiCoV, Giraffe  
829 coronavirus US/OH3-TC/2006 (EF424622.1); HCoV-229E, human coronavirus 229E  
830 (NC\_002645); HCoV-HKU1, human coronavirus HKU1 (NC\_006577); HCoV-NL63, human

831 coronavirus NL63 (NC\_005831);HCoV-OC43, human coronavirus OC43(NC\_005147); Hi-  
832 batCoV HKU10, Hipposideros bat coronavirus HKU10 (JQ989269);IBV-beaudette, beaudette  
833 coronavirus (AY692454); Human MERS-CoV, middle east respiratory syndrome  
834 coronavirus(NC\_019843.3); Human MERS-CoV EMC/2012, Human betacoronavirus  
835 2c EMC/2012 (JX869059.2); Camel MERS-CoV KSA-CAMEL-363, middle east respiratory  
836 syndrome coronavirus isolate KSA-CAMEL-363 (KJ713298); MRCoV HKU18,magpie robin  
837 coronavirus HKU18(NC\_016993); BatCoV 1A, Miniopterus bat coronavirus 1A (NC\_010437);  
838 BatCoV 1B,Miniopterus bat coronavirus 1B(NC\_010436); Mi-batCoV HKU7, Miniopterus bat  
839 coronavirus HKU7 (DQ249226); Mi-batCoV HKU8, Miniopterus bat coronavirus HKU8  
840 (NC\_010438); Mink CoV strain WD1127, Mink coronavirus strain WD1127 (NC\_023760.1);  
841 MunCoV HKU13, munia coronavirus HKU13 (FJ376622);MHV-A59, murine hepatitis  
842 virus(NC\_001846); My-batCoV HKU6, Myotis bat coronavirus HKU6 (DQ249224); NH CoV  
843 HKU19,night heron coronavirus HKU19 (NC\_016994);PEDV, porcine epidemic diarrhoea  
844 virus (NC\_003436); PHEV,porcine haemagglutinating encephalomyelitis virus  
845 (NC\_007732);Pi-BatCoV-HKU5-1, Pipistrellus bat coronavirus HKU5 (NC\_009020); PorCoV  
846 HKU15, porcine coronavirus HKU15 (NC\_016990); PRCV, porcine respiratory coronavirus  
847 (DQ811787); RbCoV HKU14, rabbit coronavirus HKU14 (NC\_017083); RatCoV parker, rat  
848 coronavirus parker(NC\_012936); Rs-batCoV HKU2, Rhinolophus bat coronavirus HKU2  
849 (EF203064); Ro-batCoV-HKU9, Rousettus bat coronavirus HKU9 (NC\_009021); Ro-batCoV  
850 HKU10, Rousettus bat coronavirus HKU10 (JQ989270);Human SARS-CoV TOR2, SARS-  
851 related human coronavirus(NC\_004718); Civet SARS-CoV SZ16, SARS-related palm civet  
852 coronavirus (AY304488); Badger SARS-CoV, SARS-related badger coronavirus  
853 CFB/SZ/94/03 (AY545919.1); SARSr-Rs-batCoV HKU3, SARS-related Rhinolophus bat

854 coronavirus HKU3 (DQ022305); Scotophilus BatCoV 512, Scotophilus bat coronavirus 512  
855 (NC\_009657); SpCoV HKU17, sparrow coronavirus HKU17 (NC\_016992); TCoV, turkey  
856 coronavirus (NC\_010800); TGEV, transmissible gastroenteritis virus (DQ443743); ThCoV  
857 HKU12, thrush coronavirus HKU12 (FJ376621); Ty-BatCoV-HKU4-1, Tylonycteris bat  
858 coronavirus HKU4 (NC\_009019); WECov HKU16, white-eye coronavirus HKU16  
859 (NC\_016991); WiCoV HKU20, wigeon coronavirus HKU20 (NC\_016995).

860 **FIG 3** Multiple alignment of the amino acid sequences of the receptor-binding motifs of the  
861 spike proteins of human and civet SARSr-CoV and the corresponding sequences of SARSr-  
862 BatCoVs in different *Rhinolophus* species. Asterisks indicate positions that have fully  
863 conserved residues. Amino acid deletions among some SARSr-BatCoVs are highlighted yellow.  
864 The five critical residues for receptor binding in human SARS-CoV, at positions  
865 442, 472, 479, 487, 491, are highlighted pink.

866 **FIG 4** Phylogenetic analyses of nsp2, nsp3, nsp5, RdRp, S, ORF3, ORF8 and N nucleotide  
867 sequences of SARSr-BatCoVs from different bat species. The trees were constructed by the  
868 maximum likelihood method using (A) GTR+G; (B) GTR+G; (C) GTR+G+I; (D) TN93+G; (E)  
869 GTR+G; (F) TN93+G (G) T92 +G (H) GTR+G substitution models respectively and bootstrap  
870 values calculated from 1000 trees. Except for ORF3 and ORF8, all trees were rooted using  
871 corresponding sequences of HCoV HKU1 (GenBank accession number NC\_006577). Only  
872 bootstrap values >70% are shown. (A) 1736 nt (B) 5019 nt (C) 908 nt (D) 2777 nt (E) 3638 nt  
873 (F) 804 nt (G) 345 nt (H) 1222 nt positions respectively were included in the analyses. The  
874 scale bars represent (A) 50 (B) 10 (C) 20 (D) 20 (E) 10 (F) 20 (zG) 10 (H) 200 substitutions per  
875 site respectively. Human and civet SARSr-CoVs are in green, SARSr-Rs-BatCoVs from *R.*

876 *sinicus* are in blue and SARSr-Rs-BatCoVs from *R. ferrumequinum* are in red. The two SARSr-  
877 Rf-BatCoV strains YNLF\_31C and YNLF\_34C detected in this study are bolded.

878 **FIG 5** (A) Bootscan (upper panel) and Simplot (lower panel) analysis using the genome  
879 sequence of civet SARSr-CoV strain SZ03 as the query sequence. Bootscanning was conducted  
880 with Simplot version 3.5.1 (F84 model; window size, 1000 bp; step, 200 bp) on a gapless nt  
881 alignment, generated with ClustalX. The red line denotes SARSr-Rf-BatCoV strain YNLF\_31C,  
882 the blue line denotes SARSr-Rs-BatCoV strain Rs3367 and the black line denotes SARSr-Rs-  
883 BatCoV strain HKU3-1. The ORF8 region with potential recombination is highlighted yellow.  
884 (B) Multiple alignment of nt sequences from genome position 27000 to 28700. Bases conserved  
885 between civet SARSr-CoV SZ03 and SARSr-Rf-BatCoVs (strains YNLF\_31C and Rf1) are  
886 marked in yellow boxes. Bases conserved between civet SARSr-CoV SZ03 and SARSr-Rs-  
887 BatCoVs (strains Rs3367 and HKU3-1) are marked in green boxes. The 29-nt deletion in  
888 human SARS coronavirus TOR2 is highlighted orange. The start codon and stop codon of ORF8  
889 are labelled with black boxes.

890 **FIG 6** Estimation of tMRCA of SARSr-CoVs based on ORF1ab (A) and nsp5 (B). The mean  
891 estimated dates were labeled. The taxa were labeled with their sampling dates.

892 **FIG 7** SARSr-Rf-BatCoV YNLF31C mRNA leader-body junction and flanking sequences. The  
893 subgenomic ORF8 mRNA sequences are shown in alignment with the leader and the genomic  
894 sequence. The start codon AUG in subgenomic RNA is depicted in red. The putative TRS is  
895 depicted in boldface type and underlined. Identical bases between leader sequence and  
896 subgenomic mRNA sequence are in blue. Identical bases between genome and subgenomic  
897 mRNA sequences are in green.

898 Table 1. Detection of CoVs in different bat species by RT-PCR of the 440-bp fragment of RdRp gene

899

Scientific name	Common name	No. of bats tested	No. of bats positive for CoV	CoV detected/closest match in GenBank	Nt identity to closest match (%)	Sampling location of positive bats
<i>Rhinolophus luctus</i>	Woolly horseshoe bat	32	0	-	-	-
<i>Rhinolophus affinis</i>	Intermediate horseshoe bat	22	0	-	-	-
<i>Rhinolophus ferrumequinum</i>	Greater horseshoe bat	11	2	SARS-CoV (2)	100	Lufeng
<i>Rhinolophus steno</i>	Lesser brown horseshoe bat	34	1	Rs-BatCoV HKU2 (1)	92	Mojiang
<i>Hipposideros pomona</i>	Pomona roundleaf bat	17	2	Hi-BatCoV HKU10 (2)	81-87	Mojiang
<i>Myotis daubentonii</i>	Daubenton's bat	98	32	My-BatCoV HKU6 (24)	78-99	Xiangyun
				Rs-BatCoV HKU2 (1)	93	Mojiang
				Rs-BatCoV HKU2 (4)	80-81	Xiangyun
				Mi-BatCoV HKU7 (2)	96	Mojiang
				Mi-BatCoV HKU8 (1)	96	Mojiang
<i>Rousettus leschenaulti</i>	Leschenault's rousette	115	9	Ro-BatCoV HKU9 (9)	75-79	Mengla
Unknown bat species		19	0	-	-	-

900 Table 2. Percentage amino acid identities of the selected predicted gene products of SARSr-CoVs to civet SARSr-CoV strain SZ3

	nsp2	nsp3	nsp5	nsp12	S	ORF3	E	M	ORF8 <sup>a</sup>	N
Civet SARSr-CoV civet007	99.5	99.5	100.0	99.7	98.6	98.1	100.0	100.0	98.3	902
Civet SARSr-CoV SZ16	100.0	99.9	100.0	99.9	99.9	100.0	100.0	100.0	98.3	100.0
Human SARS-CoV BJ01	99.8	99.6	100.0	99.9	98.8	98.1	100.0	99.5	38.2	903
Human SARS-CoV GZ02	99.8	99.8	100.0	99.9	99.0	97.8	100.0	99.5	98.3	904
Human SARS-CoV Tor2	99.8	99.6	100.0	99.9	98.6	98.1	100.0	99.5	37.3	100.0
SARSr-Rs-BatCoV Rs3367	97.8	96.8	100.0	99.6	92.3	96.7	99.1	97.7	32.2	905
SARSr-Rs-BatCoV RsSHC014	98.3	96.8	99.7	99.6	90.1	96.7	99.1	97.7	33.0	99.5
SARSr-Rs-BatCoV WIV1	97.8	96.8	99.7	99.5	92.3	96.3	99.6	97.7	32.2	906
SARSr-Rs-BatCoV HKU3-1	90.6	91.7	99.3	98.6	77.9	81.3	97.4	98.2	31.4	96.4
SARSr-Rs-BatCoV HKU3-2	90.6	91.7	99.3	98.6	77.8	81.3	96.5	98.2	31.4	907
SARSr-Rs-BatCoV HKU3-3	90.6	91.7	99.3	98.6	77.9	81.3	96.1	98.2	31.4	908
SARSr-Rs-BatCoV HKU3-6	90.6	91.7	99.3	98.5	78.0	81.3	97.4	98.2	31.4	96.4
SARSr-Rs-BatCoV HKU3-8	90.0	91.7	99.0	98.8	78.1	81.7	97.4	96.4	23.2	909
SARSr-Rs-BatCoV HKU3-12	90.4	91.7	99.3	98.9	78.1	81.7	97.4	98.2	31.4	96.2
SARSr-Rs-BatCoV HKU3-13	90.6	91.2	99.3	98.6	78.0	81.0	97.4	98.2	31.4	910
SARSr-Rs-BatCoV Rs672/2006	98.3	87.1	99.3	99.7	78.0	89.4	98.7	98.2	32.2	911
SARSr-Rb-BatCoV BM48-31/BGR	70.8	75.9	94.4	97.7	74.8	69.4	96.5	89.4		87.2
SARSr-Rm-BatCoV 279/2005	89.6	90.3	99.7	99.1	78.6	83.2	97.4	96.8	31.7	912
SARSr-Rm-BatCoV Rm1	89.5	90.0	99.3	92.4	78.7	83.2	97.8	96.8	33.0	97.4
SARSr-Rp-BatCoV Rp3	96.7	95.1	99.7	92.8	78.4	83.2	99.6	96.8	33.0	913
SARSr-Rp-BatCoV Rp/Shaanxi2011	93.6	93.0	100.0	92.3	79.0	82.1	90.0	96.4	33.0	97.9
SARSr-Cp-BatCoV Cp/Yunnan2011	90.8	97.5	100.0	92.2	78.9	89.4	97.0	98.6	31.4	914
SARSr-Rf-BatCoV Rf1	90.1	92.0	99.7	91.6	76.5	85.7	96.1	97.3	<b>80.4</b>	98.1
SARSr-Rf-BatCoV 273/2005	89.8	92.3	99.7	98.4	76.6	85.7	98.7	97.3	<b>80.4</b>	915
SARSr-Rf-BatCoV YNLF_31C	95.0	<b>97.1</b>	99.7	99.5	77.3	86.8	97.4	98.2	<b>81.3</b>	96.2
SARSr-Rf-BatCoV YNLF_34C	95.0	<b>97.1</b>	99.7	99.0	77.3	86.8	99.1	98.2	<b>81.3</b>	98.1

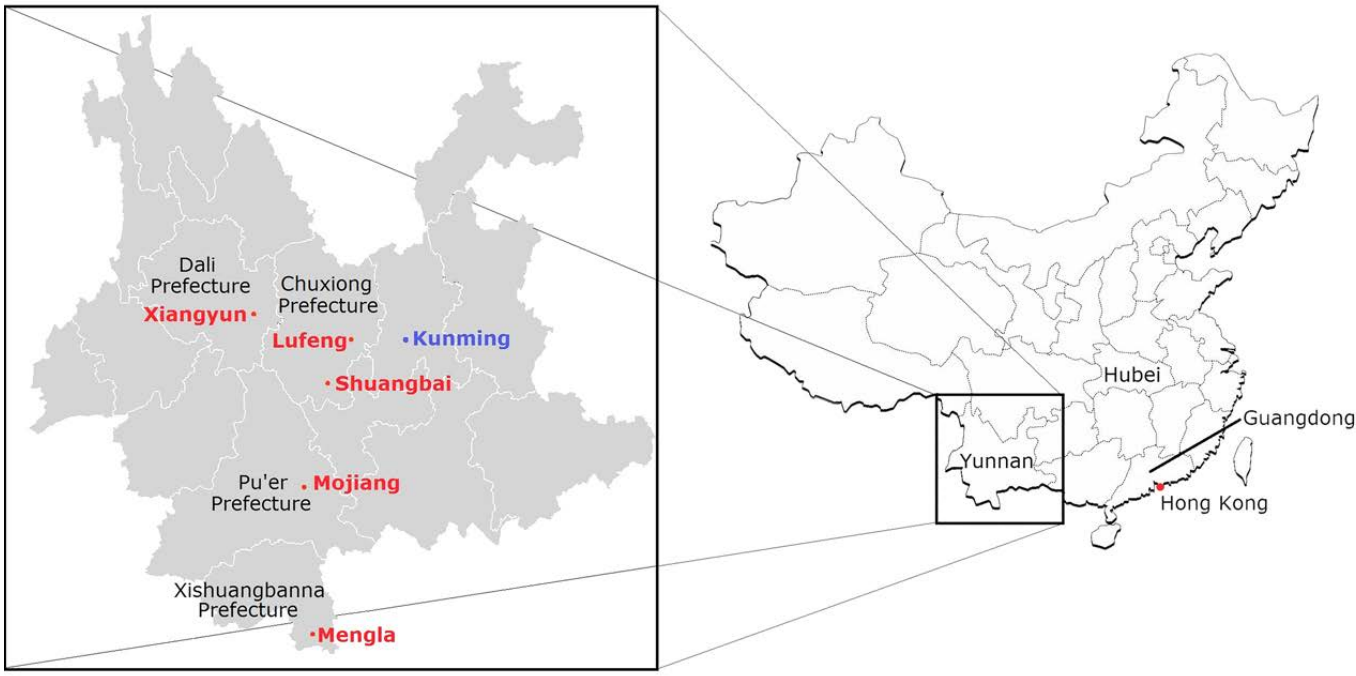
918 <sup>a</sup>The high amino acid identities in nsp3 and ORF8 between SARSr-Rf-BatCoVs and civet SARSr-CoV are in bold.

919 Table 3. Non-synonymous and synonymous substitution rates in the coding regions of SARSr-CoVs among different hosts

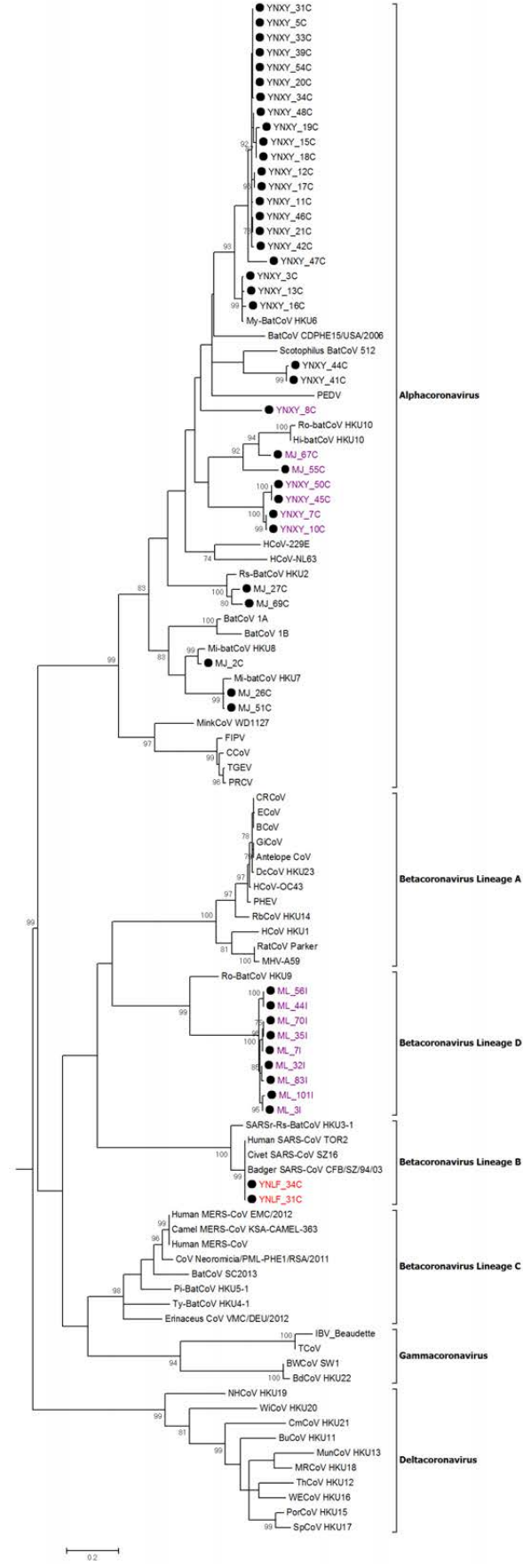
Gene	SARSr-Rf-BatCoV (n=4)			gene	SARSr-Rs-BatCoV (n=17)			gene	Civet SARSr-CoV (n=18)			gene	Human SARS-CoV (n=122)		
	Ka	Ks	Ka/Ks		Ka	Ks	Ka/Ks		Ka	Ks	Ka/Ks <sup>a</sup>		Ka	Ks	Ka/Ks
nsp1	0.013	0.081	0.161	nsp1	0.003	0.108	0.028	nsp1	0.000	0.000	—	nsp1	0.000	0.000	—
nsp2	0.036	0.349	0.103	nsp2	0.023	0.230	0.100	nsp2	0.001	0.003	0.333	nsp2	0.000	0.001	0.000
nsp3	0.030	0.414	0.073	nsp3	0.018	0.288	0.063	nsp3	0.001	0.002	<b>0.500</b>	nsp3	0.004	0.005	<b>0.800</b>
nsp4	0.012	0.391	0.031	nsp4	0.010	0.222	0.045	nsp4	0.001	0.002	<b>0.500</b>	nsp4	0.002	0.002	<b>1.000</b>
nsp5	0.003	0.442	0.007	nsp5	0.004	0.244	0.016	nsp5	0.001	0.000	—	nsp5	0.000	0.001	0.000
nsp6	0.009	0.331	0.027	nsp6	0.005	0.178	0.028	nsp6	0.000	0.002	0.000	nsp6	0.002	0.001	<b>2.000</b>
nsp7	0.018	0.549	0.033	nsp7	0.000	0.181	0.000	nsp7	0.002	0.000	—	nsp7	0.000	0.001	0.000
nsp8	0.004	0.249	0.016	nsp8	0.003	0.175	0.017	nsp8	0.001	0.000	—	nsp8	0.000	0.000	—
nsp9	0.000	0.199	0.000	nsp9	0.003	0.199	0.015	nsp9	0.001	0.000	—	nsp9	0.001	0.000	—
nsp10	0.011	0.355	0.031	nsp10	0.000	0.158	0.000	nsp10	0.000	0.000	—	nsp10	0.002	0.002	<b>1.000</b>
nsp12	0.038	0.109	0.349	nsp12	0.026	0.076	0.342	nsp12	0.000	0.003	0	nsp12	0.001	0.001	<b>1.000</b>
nsp13	0.002	0.347	0.006	nsp13	0.002	0.199	0.010	nsp13	0.000	0.003	0	nsp13	0.001	0.001	<b>1.000</b>
nsp14	0.006	0.485	0.012	nsp14	0.005	0.270	0.019	nsp14	0.001	0.003	0.333	nsp14	0.001	0.001	<b>1.000</b>
nsp15	0.016	0.452	0.035	nsp15	0.012	0.275	0.044	nsp15	0.000	0.000	—	nsp15	0.000	0.001	0
nsp16	0.008	0.306	0.026	nsp16	0.005	0.277	0.018	nsp16	0.002	0.002	<b>1.000</b>	nsp16	0.002	0.003	<b>0.667</b>
S	0.012	0.174	0.070	S	0.049	0.412	0.119	S	0.003	0.001	<b>3.000</b>	S	0.001	0.002	<b>0.500</b>
ORF3	0.012	0.065	0.185	ORF3	0.041	0.220	0.186	ORF3	0.002	0.001	<b>2.000</b>	ORF3	0.072	0.386	0.187
E	0.015	0.070	0.214	E	0.003	0.037	0.081	E	0.000	0.000	—	E	0.001	0.002	<b>0.500</b>
M	0.003	0.096	0.313	M	0.007	0.097	0.072	M	0.001	0.002	<b>0.500</b>	M	0.002	0.001	<b>2.000</b>
ORF8	0.021	0.110	0.190	ORF8	0.035	0.197	0.178	ORF8 <sup>b</sup>	0.004	0.000	—	ORF8 <sup>b</sup>	0.007	0.002	<b>3.500</b>
N	0.015	0.143	0.105	N	0.008	0.069	0.116	N	0.002	0.005	0.400	N	0.000	0.001	0

920 <sup>a</sup>Ka/Ks ratios of  $\geq 0.5$  are in bold.

921 <sup>b</sup>Only ORF8 sequences without deletions were included in analysis.







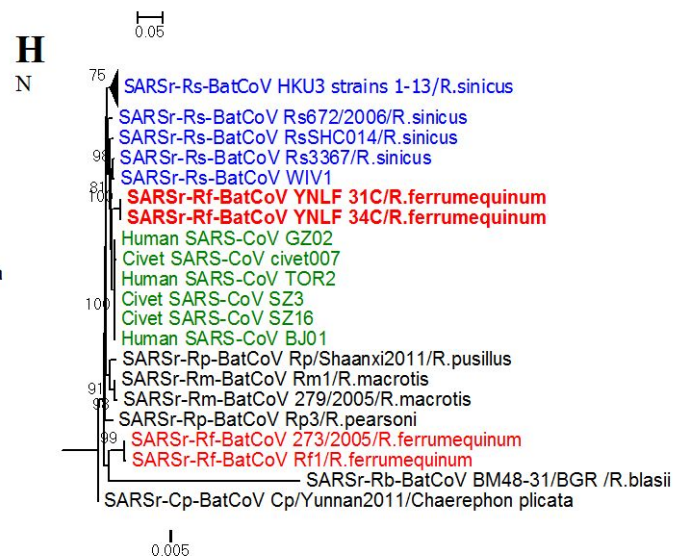
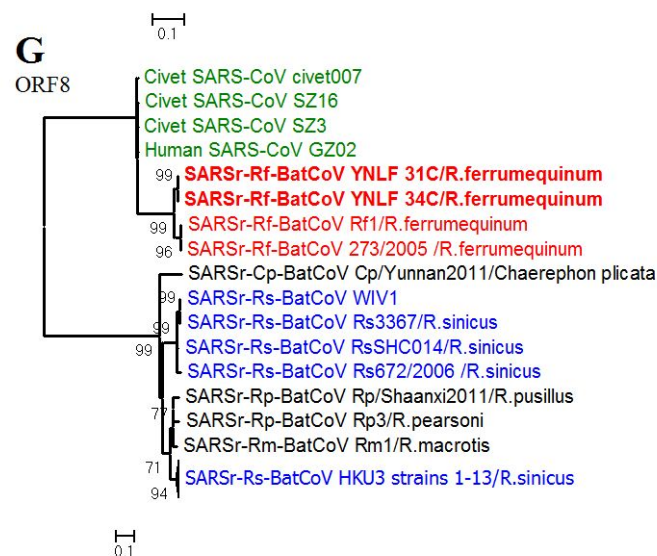
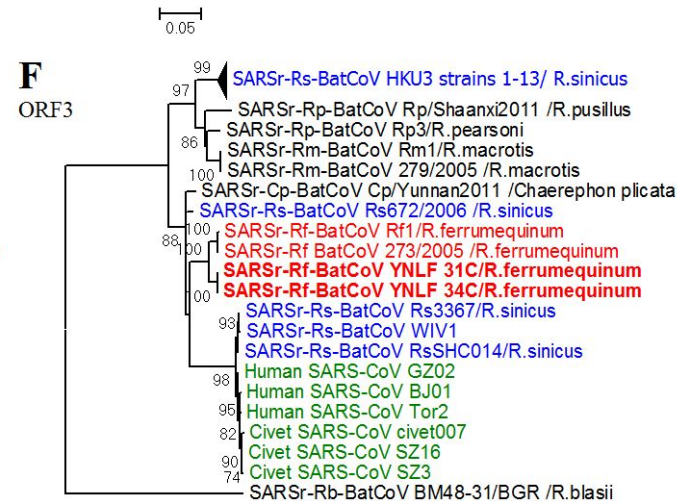
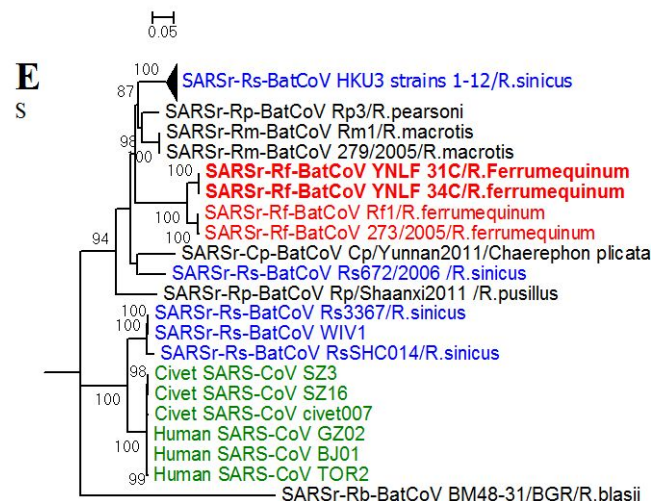
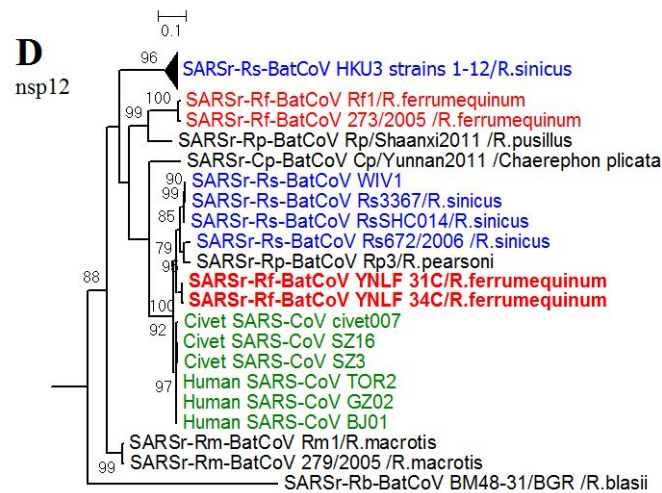
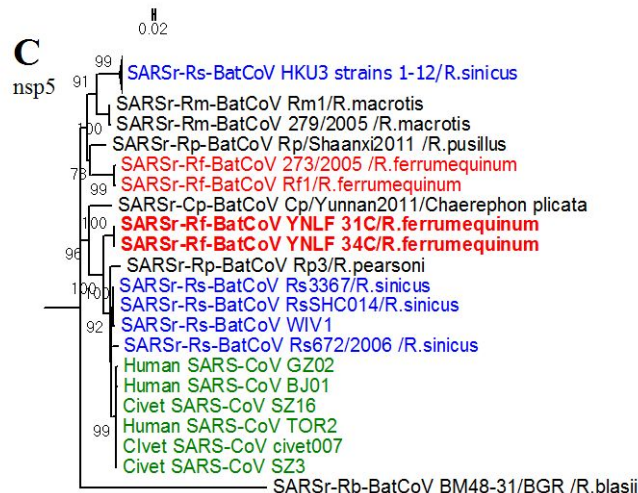
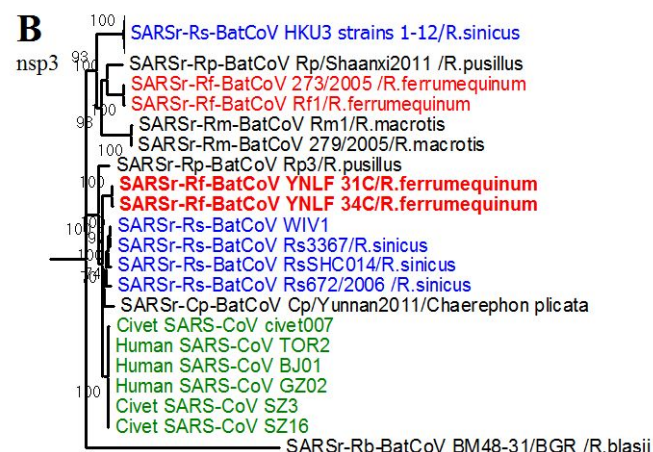
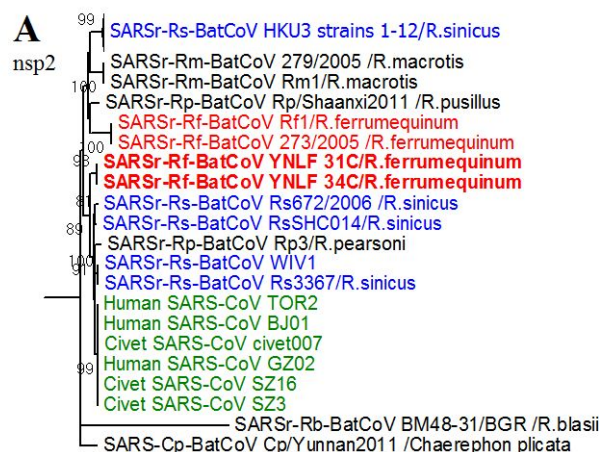
Amino acid residue position

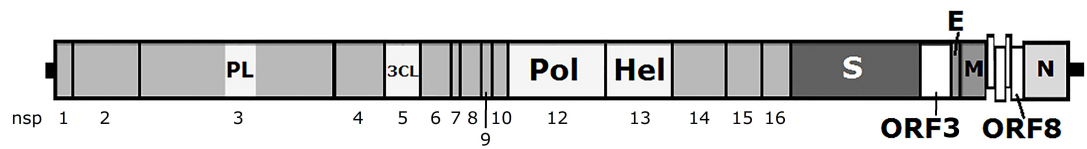
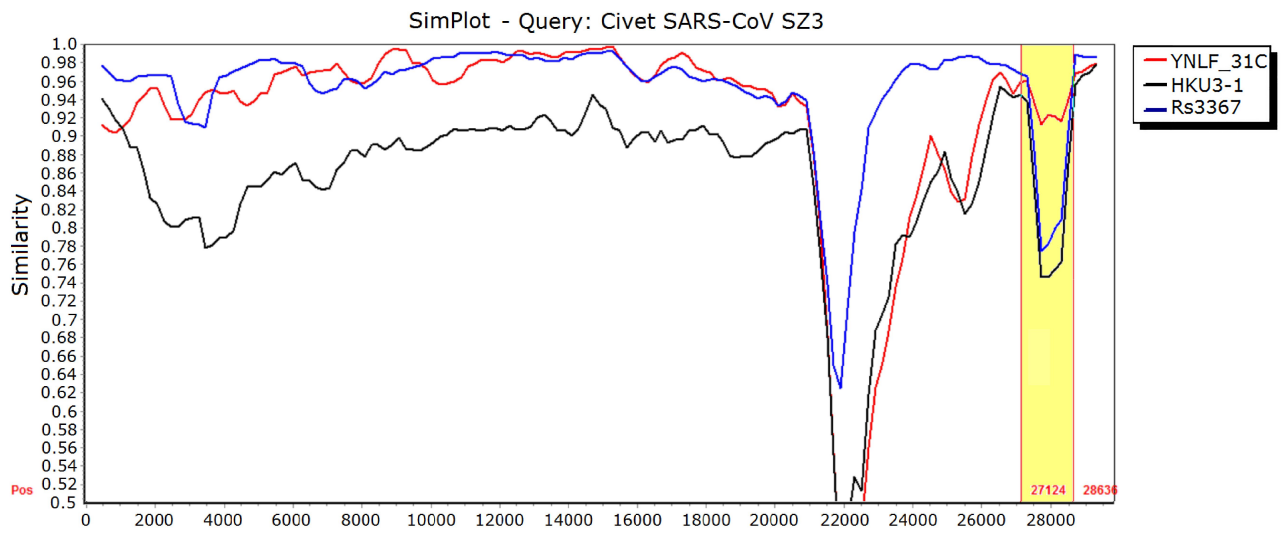
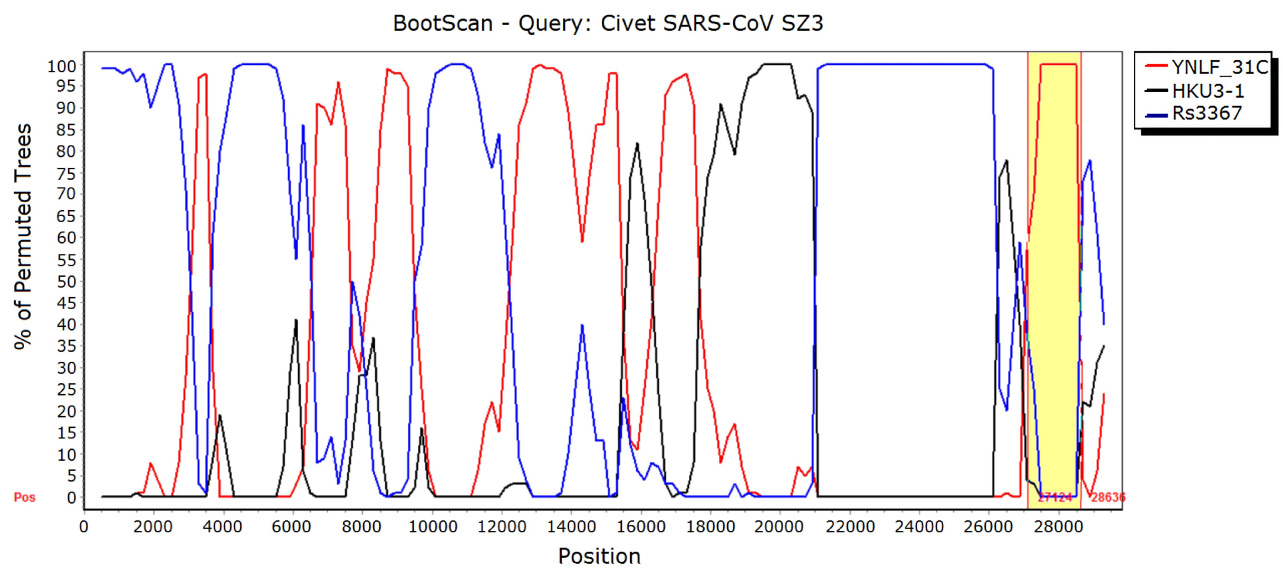
Human SARS-CoV BJ01	NTRNIDATSTGNNYKYRYLRHGKLRPFERDISNVFPSPDGKPC	PALNCYWPLNDYGFYTTTGIGYQPYR	Human	
Human SARS-CoV TOR2	NTRNIDATSTGNNYKYRYLRHGKLRPFERDISNVFPSPDGKPC	PALNCYWPLNDYGFYTTTGIGYQPYR		
Human SARS-CoV GZ02	NTRNIDATSTGNNYKYRYLRHGKLRPFERDISNVFPSPDGKPC	PALNCYWPLNDYGFYTTTGIGYQPYR		
Civet SARS-CoV SZ3	NTRNIDATSTGNNYKYRYLRHGKLRPFERDISNVFPSPDGKPC	PALNCYWPLNDYGFYTTTGIGYQPYR	Civet	
Civet SARS-CoV civet007	NTRNIDATSTGNNYKYRYLRHGKLRPFERDISNVFPSPDGKPC	PALNCYWPLNDYGFYTTTGIGYQPYR		
SARSr-Rs-BatCoV Rs3367	NTRNIDATSTGNNYKYRSLRHGKLRPFERDISNVFPSPDGKPC	PAFNCYWPLNDYGFYITNGIGYQPYR	R.sinicus	
SARSr-Rs-BatCoV RsSHC014	NTNSKDSSTSGNNYLYRWRRSKLNPYERDLSNDIYSPGGQSCSAV	PGNCYNPLRPGYFTTAGVGHQPYR		
SARSr-Rs-BatCoV WIV1	NTRNIDATSTGNNYKYRSLRHGKLRPFERDISNVFPSPDGKPC	PAFNCYWPLNDYGFYITNGIGYQPYR		
SARSr-Ra-BatCoV LYRa11	NTRNIDATSSGNNYKYRSLRHGKLRPFERDISNVFPSPDGKPC	PAFNCYWPLNDYGFYTTNGIGYQPYR	R.affinis	
SARSr-Rm-BatCoV Rm1	NTAAQD-QG	QYYYSRYRKEKLKPPFERDLS	SDE-NGVYTLSTYDFYPSIPVEYQATR	R.macrotis
SARSr-Rm-BatCoV 279/2005	NTAAQD-QG	QYYYSRYRKEKLKPPFERDLS	SDE-NGVYTLSTYDFYPSIPVEYQATR	
SARSr-Rp-BatCoV Rp3	NTAAQD-QG	QYYYSRHRKTKLPFERDLS	SDE-NGVRTLSTYDFYPSIPVEYQATR	
SARSr-Cp-BatCoV Cp/Yunnan2011	NTANQD-RG	QYYYSRKRKTKLPFERDLS	SDE-NGVRTLSTYDFYPSIPVEYQATR	R.pearsoni
SARSr-Rp-BatCoV Rp/Shaanxi2011	NTANQD-QG	QYYYSRKRKEKLKPPFERDLS	SDE-NGVYTLSTYDFYPSIPVEYQATR	Chaerephon plicata
SARSr-Rs-BatCoV Rs672/2006	NTAKQD-QG	QYYYSRKRKTKLPFERDLS	SDE-NGVRTLSTYDFYPSIPVEYQATR	R.pusillus
SARSr-Rb-BatCoV BM48-31/BGR/2008	NTNSLD-SS	NEFFYRRFRHGKIKPYGRDLSNVLFNPSGGTCS	AEGLNCYKPLASYGFTQSSGIGFQPYR	R.sinicus
SARSr-Rs-BatCoV HKU3-1	NTAKHL-TG	NYYYSRHRKTKLPFERDLS	SDDGNGVYTLSTYDFNPNVPVAYQATR	R.sinicus
SARSr-Rs-BatCoV HKU3-7	NTAKQD-TG	NYYYSRHRKTKLPFERDLS	SDDGNGVYTLSTYDFNPNVPVAYQATR	
SARSr-Rf-BatCoV Rf1	NTAKQD-VG	SYFYRSRHSKLPFERDLS	SEE-NGVRTLSTYDFNPNVPVAYQATR	
SARSr-Rf-BatCoV 273/2005	NTAKQD-VG	SYFYRSRHSKLPFERDLS	SVE-ENGRTLSTYDFNPNVPVAYQATR	R.ferrumequinum
SARSr-Rf-BatCoV YNLF 31C	NTAKYD-VG	SYFYRSRHSKLPFERDLS	SEE-NGARTLSTYDFNPNVPVAYQATR	
SARSr-Rf-BatCoV YNLF 34C	NTAKYD-VG	SYFYRSRHSKLPFERDLS	SEE-NGARTLSTYDFNPNVPVAYQATR	
Clustal Consensus	** *                      ** * * * * *			
	5 a.a deletion		12 a.a deletion	

5 a.a deletion

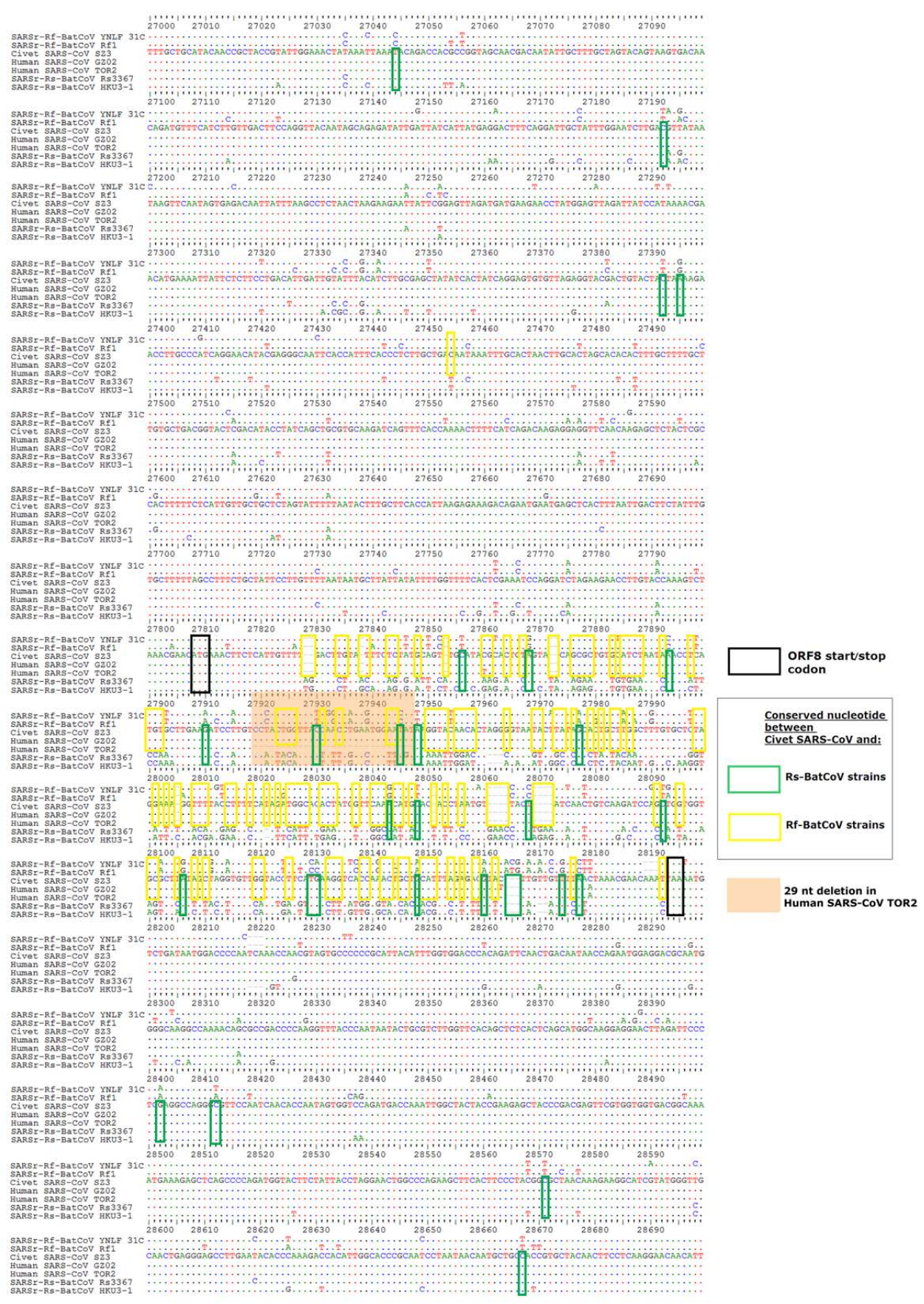
12 a.a deletion











ORF8 start/stop codon

Conserved nucleotide between Civet SARS-CoV and:

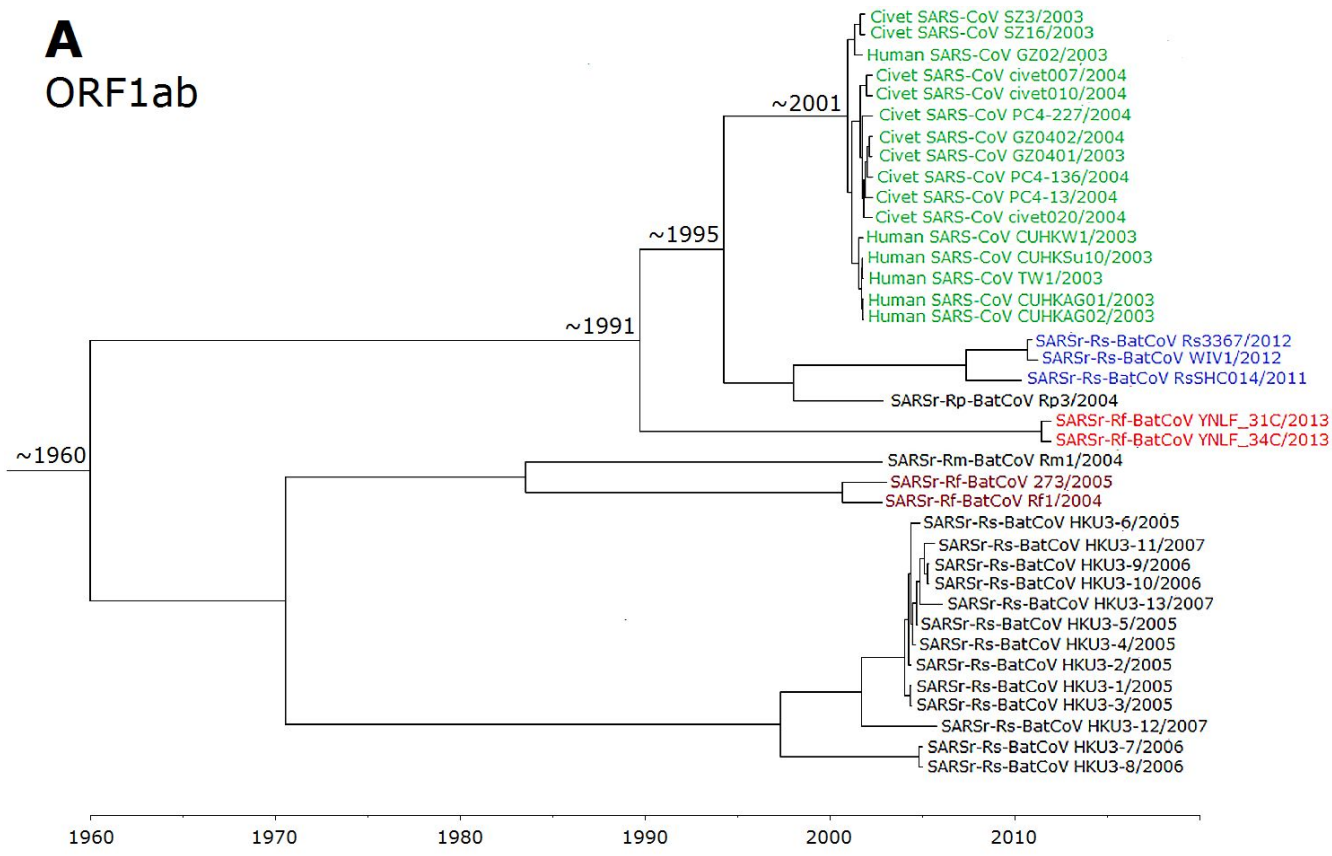
Rs-BatCoV strains  
Rf-BatCoV strains

29 nt deletion in Human SARS-CoV TOR2



**A**

ORF1ab



**B**

nsp5



leader ACCUCGAUCUCUUGUAGAUCUGUUCUUUAAACGAACUUUAAAAUCUGUGUGGCU

ORF8 mRNA ACCUCGAUCUCUUGUAGAUCUGUUCUUUAAACGAACAUGAAACUUCUCAUUGUU

genome UAUAGAAGAACCUUGUAACAAAGUCUAAACGAACAUGAAACUUCUCAUUGUU